NAVAL POSTGRADUATE SCHOOL
MONTEREY, CALIFORNIA

THESIS

A COMPARISON OF TWO COMPUTER MODELS OF SOUND PROPAGATION FOR A WEDGE SHAPED OCEAN OVER A PENETRABLE BOTTOM

by

Charles Curtis Meisenheimer

September, 1993

Thesis Advisor:	A.B. Coppens
Co-Advisor:	J.V. Sanders

Approved for public release; distribution is unlimited

REPORT DOCUMENTATION PAGE

Form approved OMB No. 0704-188

1. AGENCY USE ONLY (*Leave Blank*)	2. REPORT DATE	3. REPORT TYPE AND DATES COVERED
	September 1993	Master's Thesis

4. TITLE AND SUBTITLE
A Comparison of Two Computer Models of Sound Propagation for a Wedge Shaped Ocean Over a Penetrable Bottom

5. FUNDING NUMBERS

6. AUTHOR(S)
Meisenheimer, Charles C.

7. PERFORMING ORGANIZATION NAME(S) AND ADDRESS(ES)
Naval Postgraduate School
Monterey, CA 93943-5000

8. PERFORMING ORGANIZATION REPORT NUMBER

9. SPONSORING/MONITORING AGENCY NAME(S) AND ADDRESS(ES)

10. SPONSORING/MONITORING AGENCY REPORT NUMBER

11. SUPPLEMENTARY NOTES
The views expressed in this thesis are those of the author and do not reflect the official policy or position of the Department of Defense or the U.S. Government

12a. DISTRIBUTION/AVAILABILITY STATEMENT
Approved for public release; distribution is unlimited.

12b. DISTRIBUTION CODE

13. ABSTRACT (Maximum 200 words)

The problem of determining the acoustic pressure in a wedge shaped wave guide is examined. Two computer models, one using the method of images, the other using coupled normal modes, are compared. This comparison is over the benchmark wedge of the Acoustic Society of America. Three scenarios were examined: isovelocity water over a pressure release bottom, isovelocity water over a penetrable, lossless bottom, and isovelocity water over a penetrable, lossy bottom. In all cases good agreement was seen between both models, with some differences due to a rigid sub-bottom in the normal mode model. The strengths and weaknesses of each model is examined. An analytic solution in normal modes of the waveguide with a pressure release surface, rigid bottom, and a discontinuous speed of sound profile is presented. A brief history of research into the wedge problem is included in the introduction.

14. SUBJECT TERMS	15. NUMBER OF PAGES
Acoustic Models, Computer Models, Normal Mode Determination, Method of Images	68
	16. PRICE CODE

17. SECURITY CLASSIFICATION OF REPORT	18. SECURITY CLASSIFICATION OF THIS PAGE	19. SECURITY CLASSIFICATION OF THIS ABSTRACT	20. LIMITATION OF ABSTRACT
Unclassified	Unclassified	Unclassified	UL

NSN 7540-01-280-5500

Standard Form 298 (Rev. 2-89)
Prescribed by ANSI Std 239-18

Approved for public release; distribution is unlimited.

A Comparison of Two Computer Models of Sound Propagation for a Wedge Shaped Ocean Over a Penetrable Bottom

by

Charles Curtis Meisenheimer
Lieutenant, United States Navy
B.A., University of California, Los Angeles, 1984

Submitted in partial fulfillment of the requirements for the degree of

MASTER OF SCIENCE IN APPLIED PHYSICS

from the

NAVAL POSTGRADUATE SCHOOL
September, 1993

Author: _____
Charles Curtis Meisenheimer

Approved by: _____
Alan B. Coppens, Thesis Advisor

_____
James V. Sanders, Thesis Advisor

_____
William B. Colson, Chairman, Department of Physics

ABSTRACT

The problem of determining the acoustic pressure in a wedge shaped wave guide is examined. Two computer models, one using the method of images, the other using coupled normal modes, are compared. This comparison is over the benchmark wedge of the Acoustic Society of America. Three scenarios were examined: isovelocity water over a pressure release bottom, isovelocity water over a penetrable, lossless bottom, and isovelocity water over a penetrable, lossy bottom. In all cases good agreement was seen between both models, with some differences due to a rigid sub-bottom in the normal mode model. The strengths and weaknesses of each model is examined. An analytic solution in normal modes of the waveguide with a pressure release surface, rigid bottom, and a discontinuous speed of sound profile is presented. A brief history of research into the wedge problem is included in the introduction.

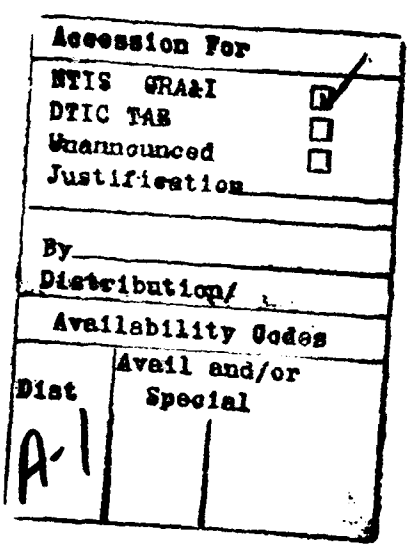

TABLE OF CONTENTS

LIST OF FIGURES

ACKNOWLEDGMENTS

First, my thanks to Professors Alan Coppens and James Sanders for providing this topic for me. The insights I have developed during this thesis research have proved very enrichening. Also, to Professor Ching-Sang Chiu for his work in his model and for graciously allowing me to use it.

Finally, I'd like to thank my wife, Cindy, for all her support during a most difficult time in my life, and to Brandie and Travis for reminding me constantly that there is life outside of school.

I. INTRODUCTION

With the recent decline in the threat of deep water submarine forces, growing emphasis is being placed on operations in relatively shallow water. In contrast to open ocean models, shallow water models of sound propagation are influenced by interaction with the bottom. Variables such as bottom composition, slope angle, sediment density, etc., make acoustic predictions difficult at best. At present there is no closed analytic solution to the problem of a penetrable, sloping bottom as found close to shorelines or along the continental shelf. However, computer models using various approximating methods are in use. Computer models are limited only by the speed and memory of the computer. With faster computers being developed, more computationally intensive models become practical. These models include the parabolic equation approximation, image theory, and adiabatic normal mode theory.

A. PARABOLIC EQUATION

By replacing the Helmholz equation with a one-way parabolic equation (PE), an acoustic field can be generated as an initial value problem. The PE method was developed for the radar community and first applied to underwater acoustics by Tappert with restrictions on the maximum angular aperture at the source [Ref 1]. Collins finally eliminated this limitation of the PE model with a higher order parabolic equation [Ref 2]. PE methods by Jensen and Kuperman [Ref 3] took advantage of improved computing power and showed valid results when compared to model tank experiments [Ref 4] for upslope propagation. This model showed modal cutoff as the sound traveled upslope. It also showed the sound propagating into the bottom at the modal cutoff depths. Jensen and Tindle used improved numerical methods to further study this problem [Ref 5].

To increase accuracy, Lee and McDaniel broke the wedge up into a number of discrete sections and applied the normal PE methods [Ref 6]. A more recent method of rotated parabolic equations by Collins has shown good results [Ref 7]. Finally, Fawcett has developed a three-dimensional computer model using PE methods combined with Fast Fourier Transform (FFT) algorithms [Ref 8].

B. METHOD OF IMAGES

Similar to the image reflections in a kaleidoscope, this method combines the contributions of the virtual sound sources to calculate the pressure field. Macpherson and Dainteth proposed a phase incoherent model for upslope propagation in 1966 using the method of images with some success [Ref 9]. Coppens *et. al.* [Ref 10] later developed a phase coherent model to calculate the pressure amplitude along the bottom of a wedge of water overlying a fast fluid bottom in the upslope direction using the incident plane wave reflection coefficient stated by Brekhovskikh and Lysenov [Ref 11]. Baek then developed a computer model of pressure throughout the water over the fast bottom [Ref 12]. However, this model was limited to a fast bottom due to the critical grazing angle of the sound to the bottom. LeSesne used the same model as a basis for a three dimensional model, which produced pressure fields in the cross slope case [Ref 13]. He further validated his computer results with experimental results from a model tank. Kaswandi then developed the model for a slow bottom in the downslope direction [Ref 14]. Concurrently, Li introduced a model which applies to both fast and slow bottoms [Ref 15]. Nassopoulos then took all the previous models under development at the Naval Postgraduate School and combined them in the computer program URTEXT [Ref 16]. Independent of this research, Buckingham and Deane developed a similar model, which produced a transmission loss plot as a function of depth and range from the source [Ref 17].

The analytic development of the method is an ongoing process. Nassopoulos implemented the use of image doublets [Ref 16]. Livingood then developed the image doublets to the three dimensional case [Ref 18]. Presently, work on Taylor expansions of sets of four images is being done by Joyce [Ref 19].

Tests done by Kim [Ref 20] and by LeSesne are cited to prove the validity of the image model. LeSesne compared his model with experimental conditions, while Kim compared his to a parabolic equation model developed by Jaeger [Ref 21] which used an implicit finite-difference solution. This turned out to be a favorable comparison.

While validated in comparisons with both other methods and with experiment, the method of images still has some flaws. It is very computer intensive, especially as the angle of the bottom becomes very shallow. Improvements include truncation of images that do not significantly contribute to the total pressure field.

C. NORMAL MODES

Normal mode theory is a range independent approach. However, for the wedge problem a range dependent model is needed. Pierce showed that an approximation of the normal modes can be used by performing an adiabatic separation of depth and range in the wave equation [Ref 22]. Graves, Nagl, Uberall, and Zarur then applied this method to the wedge problem using isospeed water over a rigid bottom [Ref 23]. This method achieved good agreement at large angles when compared to experimental values [Ref 24]. This approach was limited to large angles and a perfectly reflecting bottom. Buckingham developed a solution of the penetrable bottom. In this method he first calculates an effective pressure release bottom below the actual penetrable bottom. The depth of this bottom is a function of the density and speed of sound of the actual bottom. He then applied the sum of the normal modes to this new bottom [Ref 25].

A problem of the adiabatic normal mode approximation is that it does not adequately explain the transition to evanescent modes at cutoff depths [Ref 3]. By combining PE with adiabatic mode theory, a critical depth function was developed which agreed with the results of Jensen and Kuperman [Ref 26].

Another method is to combine ray acoustics with local modes [Ref 27], which leads to the development of intrinsic wave modes [Ref 28]. Also using beam displacement with ray theory has shown agreement with the two-way coupled mode solution in two dimensions over a penetrable lossy bottom [Ref 29].

To take into account coupling between the modes, a version of stepwise depth variations was applied to normal mode theory [Ref 30]. This method was used first by Chiu, Desaubies, and Miller [Ref 31], then by Chiu and Ehret into the development of a model of coupled normal modes [Ref 32]. The three dimensional analysis by Sagos [Ref 33] is the extent of published information on coupled normal modes, but improvements to the theory and the model are still being pursued.

II. DEVELOPMENT

A. IMAGE THEORY

In 1978, Coppens, Sanders, Iounnou, and Kawamura predicted and measured the pressure field and phase up slope along a wedge shaped bottom [Ref 10]. LeSesne implemented a model that was not dependent on up or down slope direction [Ref 13]. Further research cited earlier developed cross slope programs, giving three dimensional capability to the model. The theory behind these models is the method of images.

Coppens *et. al.* provides the complete explanation of the theory but a summary is in order. In transmission within a waveguide there is a number of interactions of acoustic rays with the guide boundaries [Ref 34, p. 427]. In image theory each ray path is replaced by an image of the source, the distance of the source from the receiver being the total distance of the actual acoustic ray. For a sloping bottom the image is placed a distance from the reflecting boundary equal to the distance of the source from the boundary perpendicular to that boundary. Figure 1 illustrates this geometry.

The phase of the image is 180° out of phase from the source if there is an interaction with a pressure release surface, as in the case of the air-water interface, and in phase for a rigid surface—a hard bottom, for example. Each interaction of the sound with the boundaries implies the existence of a new image. The final pressure at the receiver can be calculated by taking the sum of the contributions from each image.

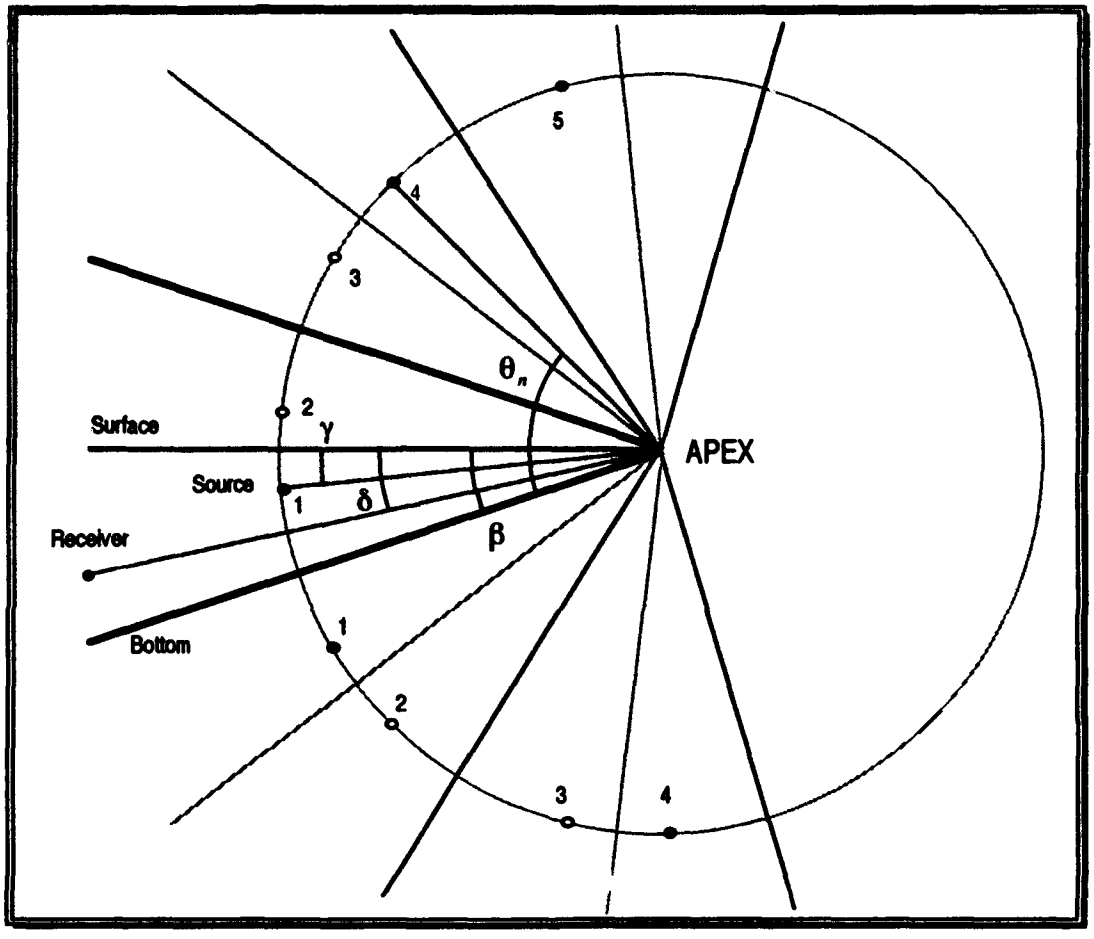

Figure 1 - Two Dimensional Wedge Geometry

For a given bottom slope angle β, the number of images N in each of the upper and lower half spaces is given by

$$N = \frac{180}{\beta} \qquad (1)$$

where β is an integer factor of 180°. Each image is numbered from the source, with the source being image number 1 for the upper half space. For the lower half space the first image below the bottom is image number 1.

Next, the grazing angle θ_n of the nth image above or below the bottom is calculated from

$$\theta_n = n\beta - \gamma \qquad \text{for } n \text{ odd} \qquad (2a)$$

$$\theta_n = (n-1)\beta + \gamma \qquad \text{for } n \text{ even} \qquad (2b)$$

where γ is the angle of the source from the surface.

The range R_n from each image to the receiver is then calculated using

$$R_n = \sqrt{r_1^2 + r_2^2 - 2r_1 r_2 \cos(\theta_n - \beta + \delta)} \qquad (3a)$$

for the upper series of images and

$$R_n = \sqrt{r_1^2 + r_2^2 - 2r_1 r_2 \cos(\theta_n + \beta - \delta)} \qquad (3b)$$

for the lower series. In these equations, r_1 is the range from the wedge apex to the source, r_2 is the range from the apex to the receiver, and δ is the angle from the surface to the receiver.

For each interaction with the surface, the reflection coefficient is -1. Each interaction with the bottom requires calculation of the reflection coefficient. This coefficient is a function of the speed of sound in each medium, the density of each medium, and the grazing angle of the ray equivalent on the bottom. It is sufficient to find the sine of this angle θ_{nm}. For this

$$\sin\theta_{nm} = \frac{r_1 \sin(\theta_n - 2m\beta) + r_2 \sin[(2m-1)\beta + \delta]}{R_n} \qquad (4a)$$

for the upper images and

$$\sin\theta_{nm} = \frac{r_1 \sin(\theta_n - 2m\beta) + r_2 \sin[(2m+1)\beta - \delta]}{R_n} \qquad (4b)$$

for the lower images [Ref 16]. Figure 2 illustrates.

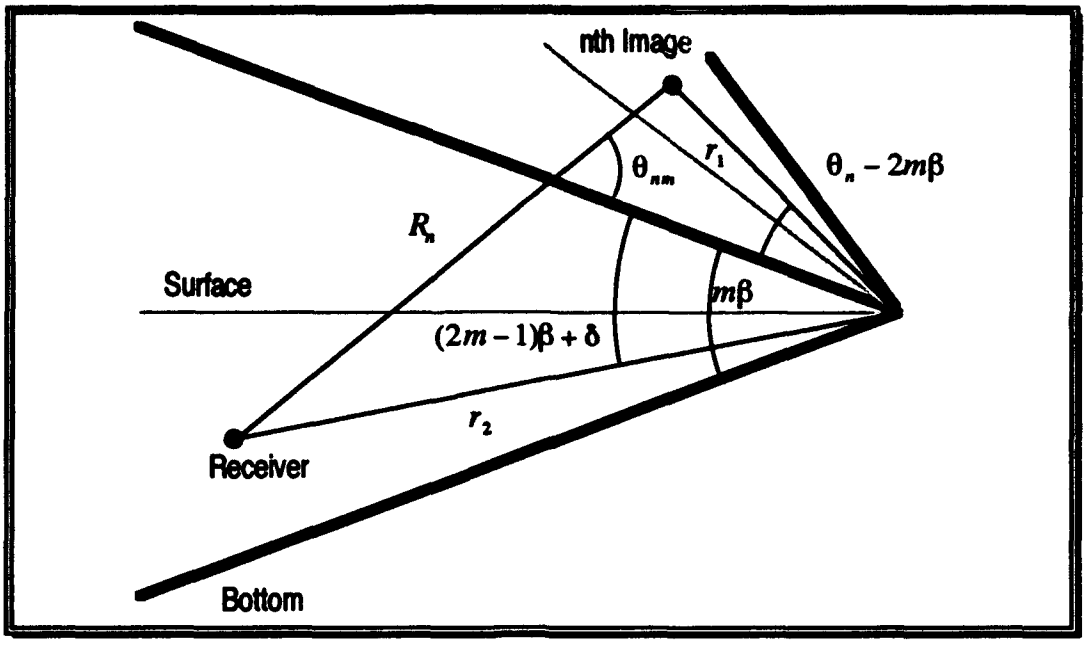

Figure 2 - Incident Angle θ_{nm} Calculation (Upper Half Space)

The reflection coefficient for each interaction $\mathbf{R}_{nm}$ then is given by

$$\mathbf{R}_{nm} = \frac{\frac{\rho_2}{\rho_1}\sin\theta_{nm} - \frac{1}{\sqrt{2}}\left(\sqrt{b^2+a^2}+a\right)^{1/2} + j\frac{1}{\sqrt{2}}\left(\sqrt{b^2+a^2}-a\right)^{1/2}}{\frac{\rho_2}{\rho_1}\sin\theta_{nm} + \frac{1}{\sqrt{2}}\left(\sqrt{b^2+a^2}+a\right)^{1/2} - j\frac{1}{\sqrt{2}}\left(\sqrt{b^2+a^2}-a\right)^{1/2}} \tag{5}$$

where ρ_1, ρ_2 are densities of the respective media, $j = \sqrt{-1}$, and a and b are given by

$$a = \left(\frac{c_1}{c_2}\right)^2 - \cos^2\theta_{nm} \tag{6a}$$

$$b = 2\left(\frac{c_1}{c_2}\right)^2 \frac{\alpha}{k_2}. \tag{6b}$$

For the above, c_1, c_2 are the speeds of sound in the respective media and α/k_2 is a measure of the bottom loss coefficient. [Ref 11]. We further define k_n as the wave number in the nth medium, where

$$k_n = \omega/c_n \tag{6c}$$

The pressure for each half space is given by summing the contribution for the upper and lower images respectively

$$\mathbf{P}_u = \sum_{n=1}^{N} \frac{1}{R_n} \exp(-jk_1 R_n)(-1)^{(n/2)} \prod_{m=1}^{M} \mathbf{R}_{nm} \tag{7a}$$

where $\prod \mathbf{R} = 1$ when n = 1,2; in (7a) and

$$\mathbf{P}_l = \sum_{n=1}^{N} \frac{1}{R_n} \exp(-jk_1 R_n)(-1)^{(n/2)} \prod_{m=0}^{M} \mathbf{R}_{nm} \tag{7b}$$

The number of interactions m with the bottom is related to the image number, so the limit M is the integer of $\left[\frac{n+1}{2}\right] - 1$ for the nth image. For convenience we have omitted the factor $e^{j\omega t}$ which would otherwise appear in (7a) and (7b).

Two special cases exist in the upper half space. For the case of the direct path of the source to the receiver (n=1), $\mathbf{R}$ is 1. In the case of a single reflection off the surface and no reflections with the bottom (n=2), $\mathbf{R}$ is again 1. The phase inversion of the ray is computed by the $(-1)^{n/2}$ term of (7a).

Since the model is frequency independent, we will scale the ranges to a distance X_c from the apex where the bottom depth is equal to the lowest normal mode cutoff depth when the bottom is fast (*i.e.*, when the sound speed ratio is less than 1). This cutoff distance is calculated by

$$k_1 X_c = \frac{\pi}{2 \sin\theta_c \tan\beta} \qquad \theta_c = \cos^{-1}\left(\frac{c_1}{c_2}\right) \tag{8a}$$

For a slow bottom an analogous scaling, convenient for the computer program is

$$k_1 X_c = \frac{\pi}{2 \tan\theta_s \tan\beta} \qquad \theta_s = \cos^{-1}\left(\frac{c_2}{c_1}\right) \tag{8b}$$

For the total pressure at the receiver, the upper and lower contributions are combined, thus

$$\mathbf{P} = \mathbf{P}_u + \mathbf{P}_l \tag{9}$$

B. COUPLED MODE THEORY

Normal mode theory describes sound propagation as a collection of eigenfunctions, called normal modes, which are determined by the depth of the sound channel boundaries and the source depth. Coupling between the modes (energy transfer) in the horizontal direction occurs due to changes in sound speed, density, or bathymetry. The Chiu-Ehret model [Ref 32] determines the pressure field using numerical evaluations. Sagos [Ref 33] modified this model for three dimensions.

Chiu [Ref 35] then developed a model in MATLAB™ called BBCM. In this model the spectral pressure at the receiver is decomposed by an FFT algorithm. At each point in the pressure field and at each frequency, the amplitude envelope for each existing normal mode is calculated, then coupled to determine the total pressure by

$$\mathbf{P}(r,z,t) = \int_{-\infty}^{+\infty} S(f) \sum_{n=1}^{N} \frac{r_0}{\sqrt{r}} U_n(r;f) Z_n(z;r,f) \exp\left\{ i\left(\int_0^{2\pi} k_n(r';f)dr - 2\pi ft \right) \right\} dt \tag{10}$$

where $S(f)$ is the source amplitude spectrum, Z_n is a linear combination of the normal modes, and $U_n(r;f)$ is the amplitude slowly varying modulation complex envelope. It is in this calculation that the coupling of the normal modes occurs.

In the MATLAB™ version, it has several advantages:

- Can handle both discrete and broad band signals defined by $S(f)$,
- The bottom can be varied—not limited to a smooth slope,
- FFT algorithms are extremely fast. Pressure fields are calculated in a fraction of the time that would be taken by URTEXT.

BBCM uses a rigid bottom for the waveguide, while in the upcoming comparison no such bottom is assumed. Therefore, the effect of this rigid bottom on the sound in the water column must be examined.

C. THE TWO LAYER WAVE GUIDE

Figure 3 shows a sound velocity profile of a hypothetical wave guide. In this guide the boundary conditions are a pressure release surface and a rigid bottom, with a discontinuous change in sound speed at depth L.

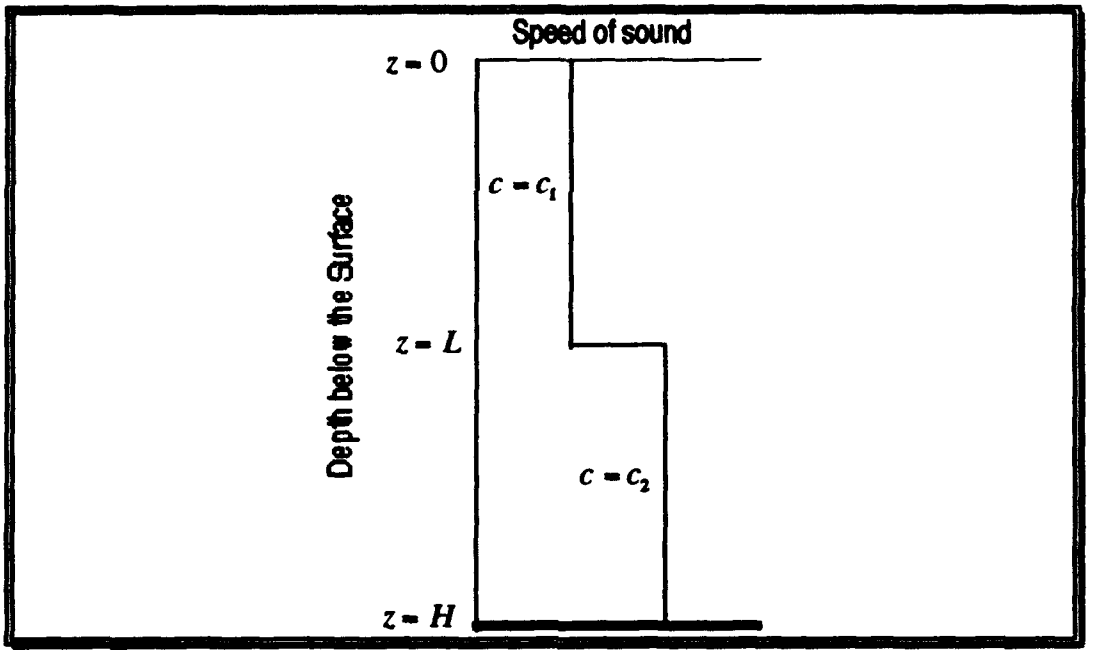

Figure 3 - Sound Velocity Profile for Comparison

Normal mode theory produces an exact solution to the normalized Helmholtz equation for sound pressure **P**. This equation, given in cylindrical coordinates for a point source, is

$$\frac{1}{r}\frac{\partial}{\partial r}\left[r\frac{\partial}{\partial r}\right]\mathbf{P}+\frac{\partial^2}{\partial z^2}\mathbf{P}+\left[\frac{\omega}{c(z)}\right]^2\mathbf{P}=\frac{2}{r}\delta(r)\delta(z-z_0)e^{j\omega t} \tag{11}$$

and has a solution of

$$\mathbf{P}(r,z,t)=-j\pi e^{j\omega t}\sum_n Z_n(z_0)Z_n(z)\left[H_0^{(2)}(\kappa_n r)\right] \tag{12}$$

where $Z_n(z)$ is the depth dependent normal mode, z_0 is the depth of the source, r is the range from the source, κ_n is the horizontal propagation constant of the nth normal mode,

and $H_0^{(2)}$ is the Hankel function where $H_0^{(2)} = J_0 - jY_0$ [Ref 34, p. 431]. The function $Z_n(z)$ is a solution to the homogeneous Helmholtz equation

$$\frac{d^2}{dz^2} Z_n + k_{zn}^2 Z_n = 0 \tag{13}$$

First we examine the case where $H = \infty$. $Z_n(z)$ must satisfy the boundary conditions of $Z(0)=0$, continuity of particle velocity and pressure across the interface at $z = L$, and $Z_n(z)$ must approach zero as z goes to infinity.

For the above conditions, we guess at two functions Z_{1n} and Z_{2n} to represent $Z_n(z)$,

$$Z_{1n}(z) = A_n \sin(k_{1zn} z) \qquad 0 \le z \le L \tag{14}$$

and

$$Z_{2n}(z) = B_n e^{-\beta_n (z-L)} \qquad L < z \tag{15}$$

where k_{1zn} is the vertical wave number of the nth depth dependent normal mode in the upper layer and β_n is the vertical propagation number of the exponential function in the lower layer. The numbers k_{1zn} and β_n are related by the equation

$$\kappa_n^2 = \left(\frac{\omega}{c_1}\right)^2 - k_{1nz}^2 = \left(\frac{\omega}{c_2}\right)^2 + \beta_n^2 \tag{16}$$

Evaluation of (14) at the surface proves that it is a valid solution, but the behavior of the functions at the interface of $z = L$ needs to be determined. At the interface, continuity of sound pressure and normal particle velocity must hold. Therefore,

$$A_n \sin(k_{1zn} L) = B_n \tag{17}$$

and

$$A_n k_{1zn} \cos(k_{1zn} L) = -B_n \beta_n \tag{18}$$

Combining (17) and (18) and manipulating gives the transcendental equation

$$\tan(k_{1zn}L) = -\frac{k_{1zn}L}{\beta_n L} \tag{19}$$

which, by defining

$$y = k_{1nz}L \tag{20}$$

and

$$a^2 = L^2\left[\left(\frac{\omega}{c_1}\right)^2 - \left(\frac{\omega}{c_2}\right)^2\right] \tag{21}$$

yields

$$\tan y = -\frac{y}{\sqrt{a^2 - y^2}} \tag{22}$$

This equation can be used to solve for k_{1zn}, and this yields β_n and κ_n, when $y < a$. Normalization of $Z_n(z)$ then produces the terms A_n and B_n, giving the final solution to (13). This solution corresponds to an oscillatory function above L overlying a function which decays exponentially as z increases. An example, $Z_2(z)$, at a frequency somewhat above cutoff, is shown in Figure 4. As can be seen, the sound energy is trapped in the upper layer with some energy leaking into the bottom.

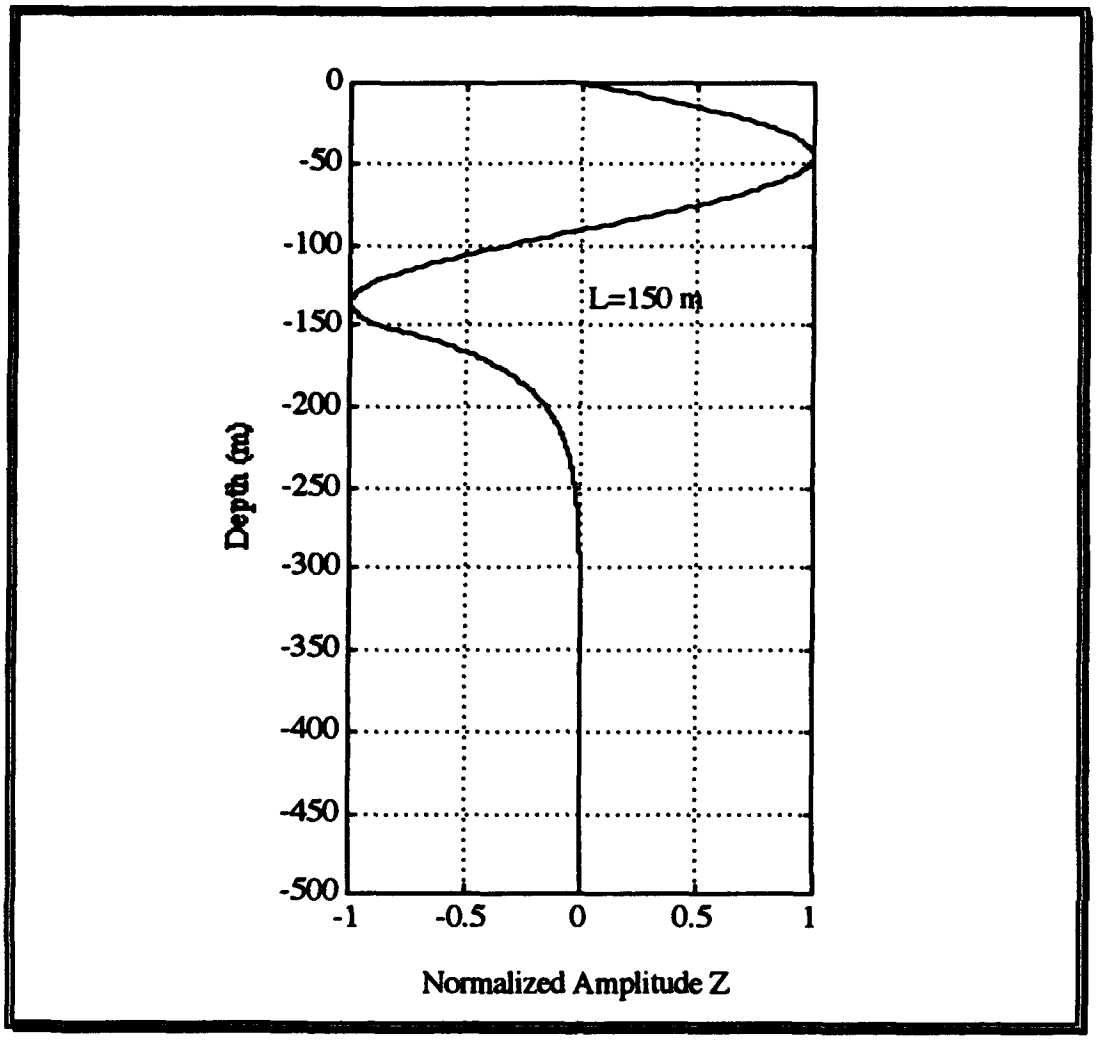

Figure 4 - Fluid Layer Overlying an Infinite Bottom

The cutoff frequency of each normal mode can be determined at each point where a_n approaches an asymptote of tan y in (22), or where

$$a_n = \frac{\pi}{2}, \frac{3\pi}{2}, \ldots, \frac{(2n-1)\pi}{2} \qquad n = 1, 2, 3, \ldots \qquad (23)$$

Substitution of (21) into (23) and manipulation yield a cutoff angular frequency of normal mode n,

$$\omega_n = \frac{(2n-1)\pi c_1 c_2}{2L\sqrt{(c_2^2 - c_1^2)}} \qquad (24)$$

We now examine the case where there is a rigid bottom at $z = H$. The solutions of the Helmholtz equation now must fulfill the additional boundary condition $\left.\frac{dZ(z)}{dz}\right|_{z=H} = 0$

For the revised boundary conditions, we choose

$$Z_{1n}(z) = A_n \sin(k_{1zn} z) \qquad 0 \le z \le L \qquad (25)$$

and

$$Z_{2n}(z) = B_n \cosh[\beta_n (H - z)] \qquad L < z \le H \qquad (26)$$

The hyperbolic cosine was chosen in analogy with the exponential choice in the previous case. It satisfies the boundary conditions at $z = H$.

Next is evaluation of (25) and (26) at the interface of $z = L$. At the interface,

$$A_n \sin(k_{1zn} L) = B_n \cosh[\beta_n (H - L)] \qquad (27)$$

and

$$A_n k_{1zn} \cos(k_{1zn} L) = -B_n \beta_n \sinh[\beta_n (H - L)] \qquad (28)$$

Combining (27) and (28) gives

$$\tan(k_{1zn} L) = -\frac{k_{1zn} L \coth[\beta_n (H - L)]}{\beta_n L} \qquad (29)$$

which, by substitution of y and a yields

$$\tan y = -\frac{y \coth\left[\left(H/L - 1\right)\sqrt{a^2 - y^2}\right]}{\sqrt{a^2 - y^2}} \qquad (30)$$

This equation can be used to solve for k_{1zn} and then β_n and κ_n can be obtained. When $y<a$ the solution is similar to that for the infinite bottom condition in that it corresponds to an oscillatory function above L and decays as z increases from L to H. The sound energy in this case is trapped in the upper layer with some leakage into the lower layer (Figure 5).

Note that, from (30), as H decreases to L, y decreases to $(n-1/2)\pi$ for $n = 1, 2, 3, \ldots$ and the normal modes will tend to approach those for a singe layer waveguide with a rigid bottom and a pressure release surface.

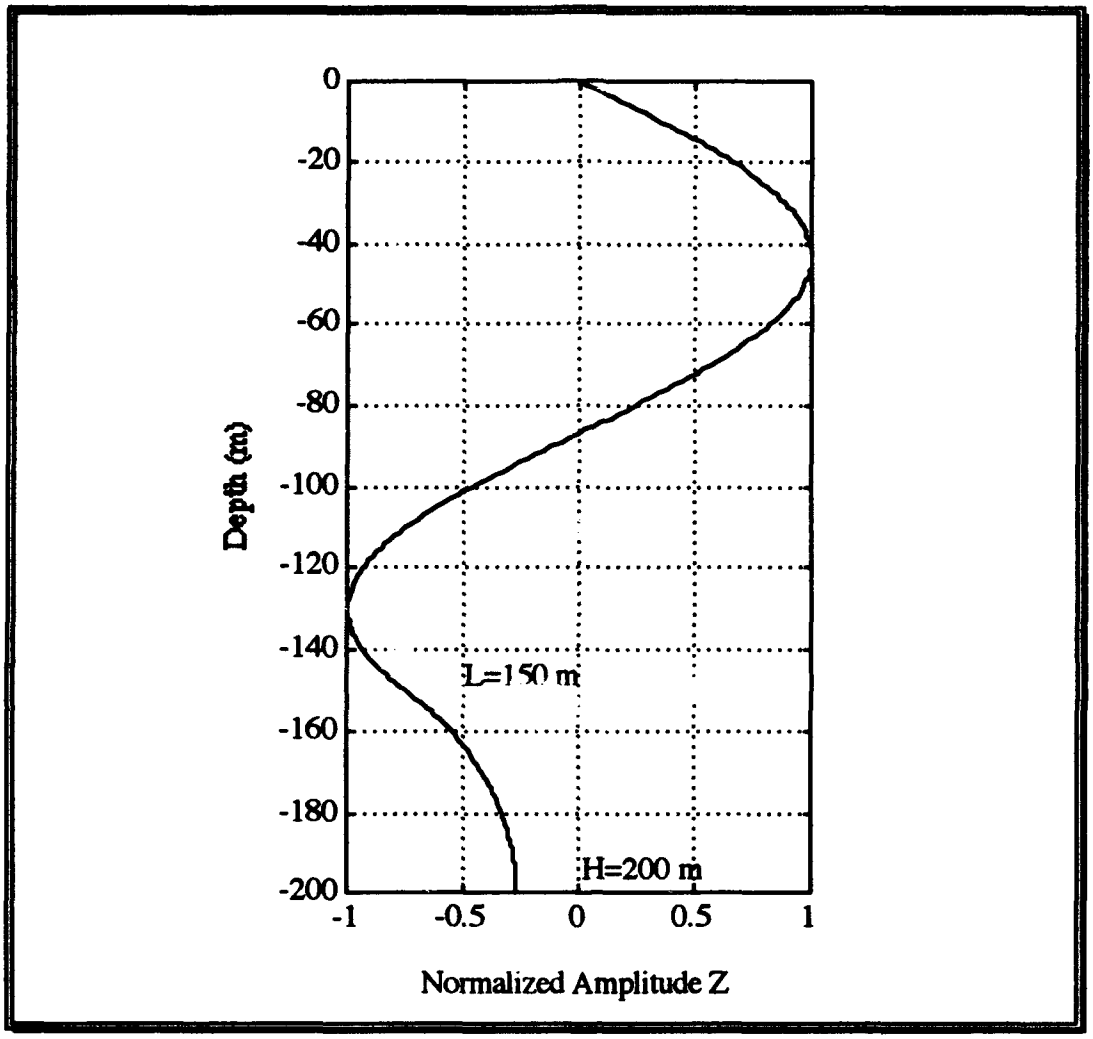

Figure 5 - Two Layers Overlying a Rigid Sub-bottom

The propagation of the normal mode exists in three regimes dependent upon k_{1zn}. We determine β_n in terms of k_{1zn} from (16) to be

$$\beta_n^2 = \left[\left(\frac{\omega}{c_1}\right)^2 - \left(\frac{\omega}{c_2}\right)^2\right] - k_{1zn}^2 \qquad (31)$$

If $k_{1zn}^2 < \left(\frac{\omega}{c_1}\right)^2 - \left(\frac{\omega}{c_2}\right)^2$, this is equivalent to $y < a$, and therefore (25) through (30) hold. If $y > a$ then β_n becomes imaginary and $Z_{2n}(z)$ becomes

$$Z_{2n}(z) = -B_n \cos\left[k_{2zn}(H - z)\right] \tag{32}$$

where k_{2zn} is defined by

$$k_{2zn}^2 = k_{1zn}^2 - \left[\left(\frac{\omega}{c_1}\right)^2 - \left(\frac{\omega}{c_2}\right)^2\right] \tag{33}$$

and is related to κ_n by

$$\kappa_n^2 = \left(\frac{\omega}{c_2}\right)^2 - k_{2zn}^2 \tag{34}$$

By applying the boundary contains to (25) and (32) and making the appropriate substitutions for y and a we produce

$$\tan y = -\frac{y \cot\left[\left(H/L - 1\right)\sqrt{y^2 - a^2}\right]}{\sqrt{y^2 - a^2}} \tag{35}$$

This equation describes a normal mode trapped in the waveguide with a pressure release surface and a rigid bottom. How that mode propagates is dependent upon κ_n.

From (16), if $\left(\frac{\omega}{c_1}\right)^2 - \left(\frac{\omega}{c_2}\right)^2 < k_{1zn}^2 < \left(\frac{\omega}{c_1}\right)^2$, then κ_n is real, and the mode propagates horizontally in the overall waveguide. If $\left(\frac{\omega}{c_1}\right)^2 < k_{1zn}^2$, κ_n becomes imaginary. The normal mode thus decays as it propagates horizontally. Figure 6 shows the vertical component of the normal mode which satisfies (35).

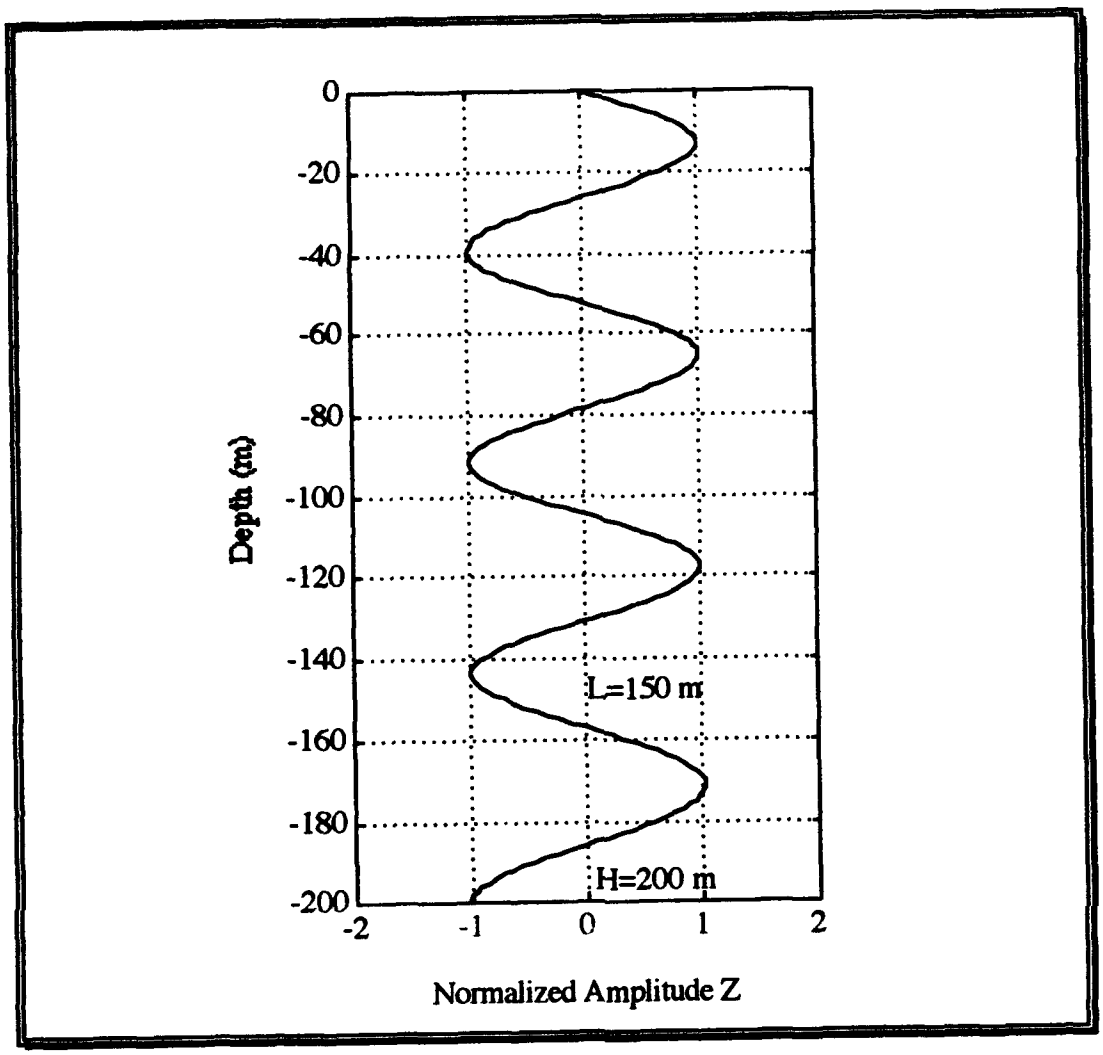

Figure 6 - Two Layers Overlying a Rigid Sub-bottom

The condition where β_n becomes imaginary is the major difference between the infinite bottom and the rigid, finite bottom. In the infinite bottom case, decreasing the layer depth L decreases the number of modes which can be propagated. However, the finite bottom adds a propagation mode throughout waveguide which must be corrected if an accurate comparison is to be made.

Another difficulty encountered is that the above discussion is valid only when all interfaces are parallel. With parallel layers, the grazing angle θ is easily computed. With a

sloping interface $L=f(r)$ this angle changes with range. It can be approximated numerically, but no analytic solution exists.

To extend to a sloping interface in a waveguide consisting of two layers with a rigid bottom of depth H and fluid interface at depth L, all the normal modes with cutoff frequencies below the frequency of the source are excited and propagate according to (25) and (26). As the sound goes upslope, each normal mode approaches its first transition depth where $\beta_n = 0$ and the pressure amplitude of the exponential function becomes uniform over the entire lower layer (Figure 7). After the transition, the normal mode now behaves sinusoidally with depth in both layers (Figure 6). As L continues to decrease, the mode approaches the second transition point, where κ_n becomes imaginary and the mode becomes evanescent in the horizontal plane.

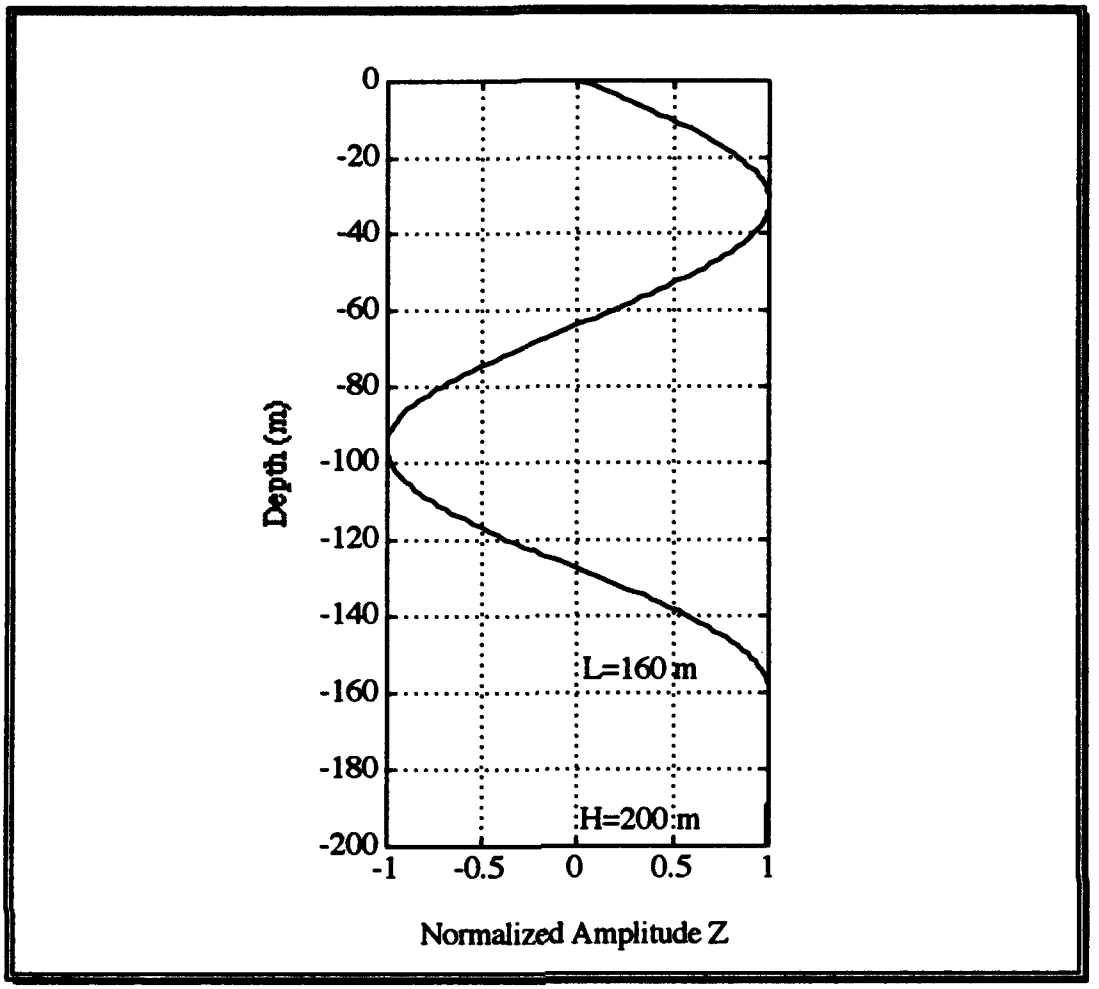

Figure 7 - Fluid Layer over a Rigid Bottom at First Transition

III. PROCEDURES AND RESULTS

A. PROCEDURES

For this research, the image model (URTEXT) and the coupled mode model (BBCM) were compared for the upslope case. Both models were run using MATLAB™, with URTEXT being translated from FORTRAN. Validation of this translation appears in Appendix A.

The parameters chosen were the benchmark wedge problem of the Journal of the Acoustic Society of America [Ref 36] (Figure 8). The speed of sound in the water is uniform at 1500 m/s and the standard seawater density of 1.021 g/cm^3 is used. A point source transmitting a continuous wave at 25 Hz is located 4 km from the apex of the wedge and 100 m below the surface. The bottom slopes at 2.86°. The composition of the bottom will be varied to test different scenarios.

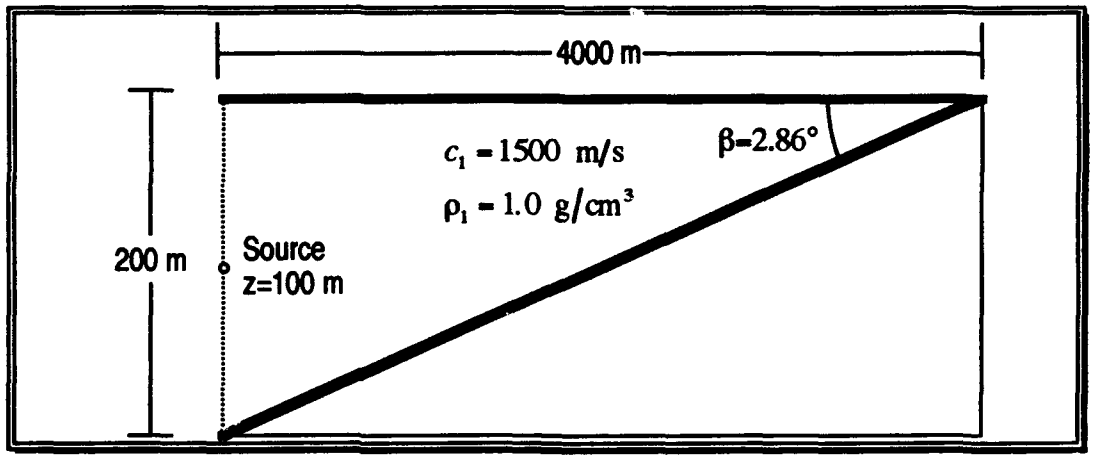

Figure 8 - JASA Benchmark Wedge

Three cases were run for comparisons. Scenario 1 uses a pressure release bottom, Scenario 2 has a fast bottom with no absorption loss, and Scenario 3 uses the same bottom with some absorption. Parameters for the environments are given in Table 1.

TABLE 1 - ENVIRONMENTAL PARAMETERS

	Scenario 1	Scenario 2	Scenario 3
c_1 (m/s)	1500	1500	1500
c_2 (m/s)	343	1700	1700
ρ_1(g/cm^3)	1.021	1.021	1.021
ρ_2(g/cm^3)	0.00121	1.500	1.500
α (dB/λ)	0.00	0.00	0.5

One difficulty was the difference in measured values between the two models. BBCM uses SI units and produces transmission loss (among other values) in dB. URTEXT uses dimensionless parameters scaled to the dump distance determined by (8a) and produces a dimensionless pressure amplitude. This can be converted to dB by

$$TL = 20\log\left(|\mathbf{P}|/X_c\right) \tag{36}$$

where TL is the transmission loss in dB, $\mathbf{P}$ is the dimensionless complex pressure, and X_c is the dimensionless dump distance. For each scenario, it was necessary to convert the SI units into the dimensionless input units for URTEXT. Actual numbers will be given later.

BBCM uses input files which model the environment. These files define the overall waveguide (water column and underlying bottom) by describing the sound velocity profile, density profile, receiver ranges, receiver depths, attenuation of each normal mode, and source amplitude spectrum [Ref 35]. Depending upon the degree of resolution desired, these input files can get quite large. A program, SCENEGEN, was written to develop these input files specifically for the two dimensional wedge.

Another problem of BBCM concern the rigid bottom of the overall waveguide. As seen from the development in Chapter II this rigid waveguide floor affects the sound in the water. Depending on the overall depth of the waveguide, free propagating normal modes of the entire waveguide are excited which are coupled with the modes which are trapped only in the water layer. These free normal modes must be identified and eliminated for accurate results.

This could be done by applying a range dependent attenuation coefficient for each normal mode, so the mode is attenuated by the bottom after it reaches its first transition point. However, BBCM does not support this. The attenuation vector that is entered in the model is range independent. Therefore, the effects of the rigid sub-bottom cannot be eliminated for this problem.

B. SCENARIO 1–PRESSURE RELEASE BOTTOM

A pressure release bottom was simulated for both models. Since both models are incapable of running if either c_2 or $\rho_2 = 0$, an air-water interface was deemed sufficient for the bottom. Inputs for URTEXT are given in Table 2. As the sound goes closer to the apex, adiabatic theory predicts less pressure as cutoff depth for each successive normal mode is reached. The actual outputs are seen in Figure 9.

TABLE 2 - URTEXT INPUTS FOR COMPARISONS

	Scenario 1	Scenario 2	Scenario 3
β	3.0°	2.86°	2.86°
γ	1.43°	1.43°	1.43°
c_1/c_2	4.412	0.8824	0.8824
ρ_1/ρ_2	850	0.6667	0.6667
X_c	69.87 m	638 m	638 m
r_1	57.33 X_c	6.27 X_c	6.27 X_c
α/k_2	0.0001 dB	0.0001 dB	0.07963 dB

For the inputs from Table 2, normal mode theory for a rigid bottom predicts seven modes will be excited by the source. But since the source is located at the pressure node of the even numbered modes, these modes are not excited. Therefor, only four modes are excited and cutoff points for these modes should be observed. The URTEXT results show these predicted characteristics, with cutoff points for the first mode at 3400 m, the third mode at 2200 m, and the fifth mode at 1000 m. Cutoff for the seventh mode cannot be seen due to the high density of contour lines in Figure 9. Further information is seen in the transmission loss plots of Figures 10 through 13.

BBCM did not produce usable data for this scenario. This is not surprising, when one considers the original purpose of the model. BBCM was written for acoustic tomography calculations. As such, the pressure release case is not considered, since there are no actual pressure release bottoms in the ocean. The model ends up taking the sound from the water column and trapping it in the underlying bottom.

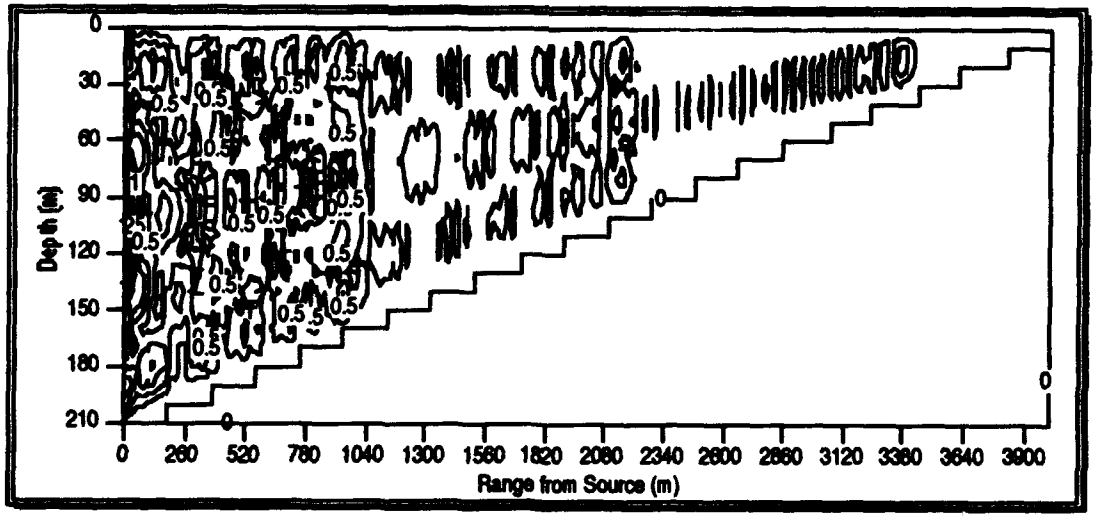

Figure 9 - Scenario 1 - URTEXT Transmission Loss in dB re 1 m

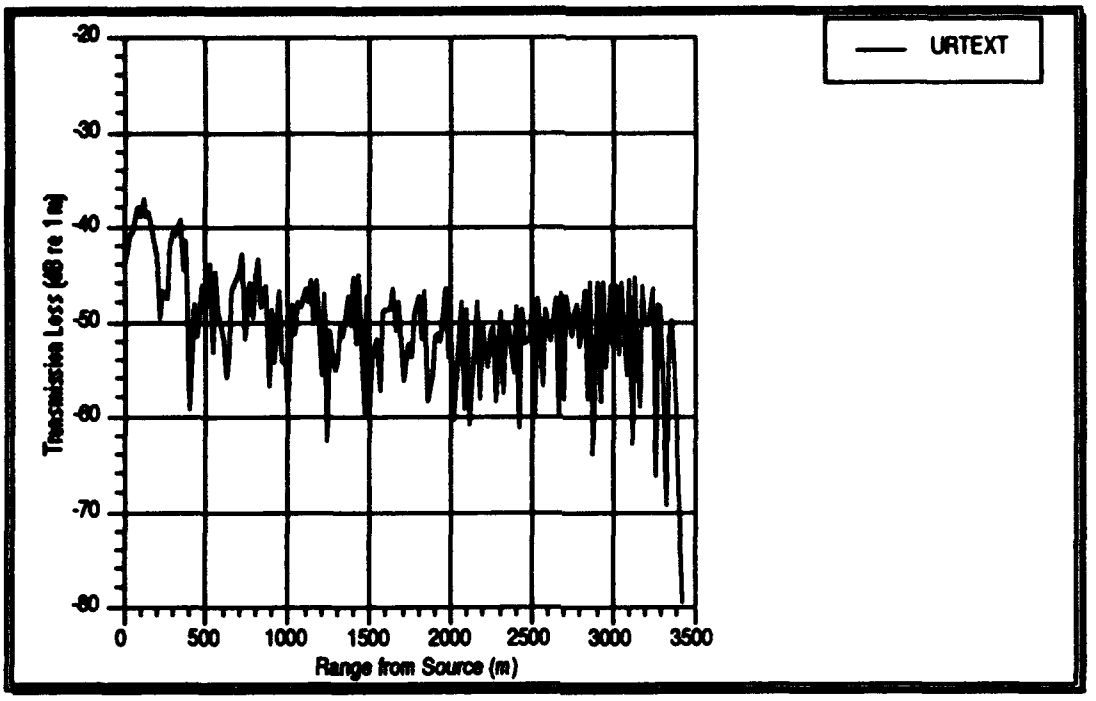

Figure 10 - Scenario 1 - 30 m Receiver

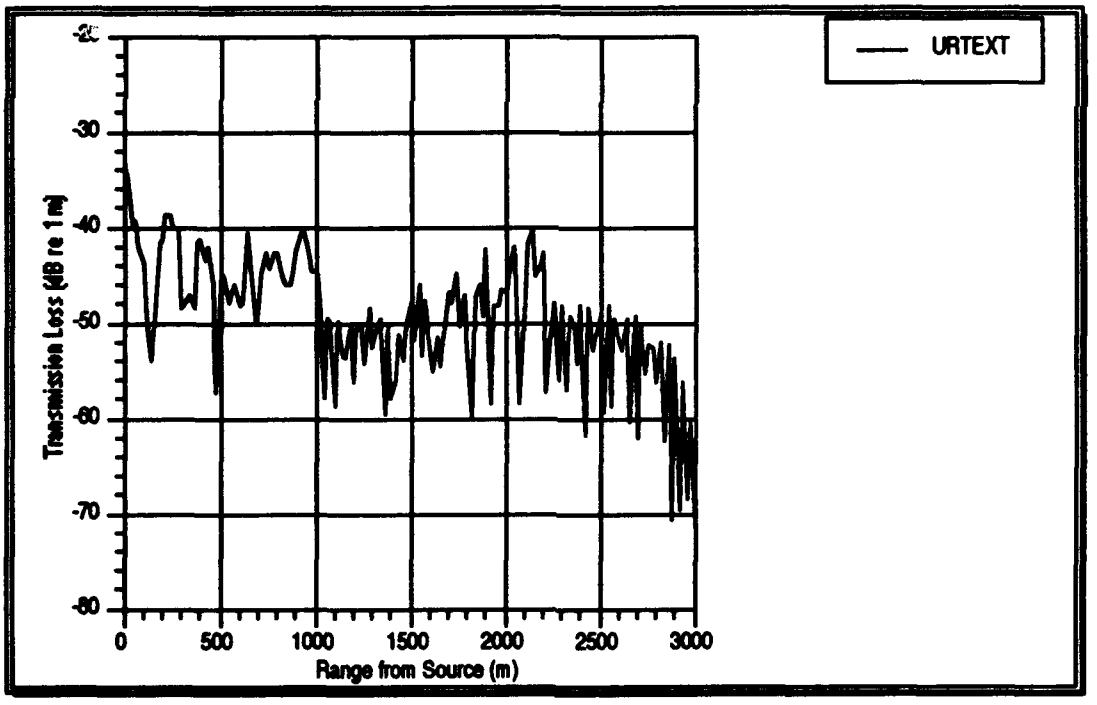

Figure 11 - Scenario 1 - 50 m Receiver Depth

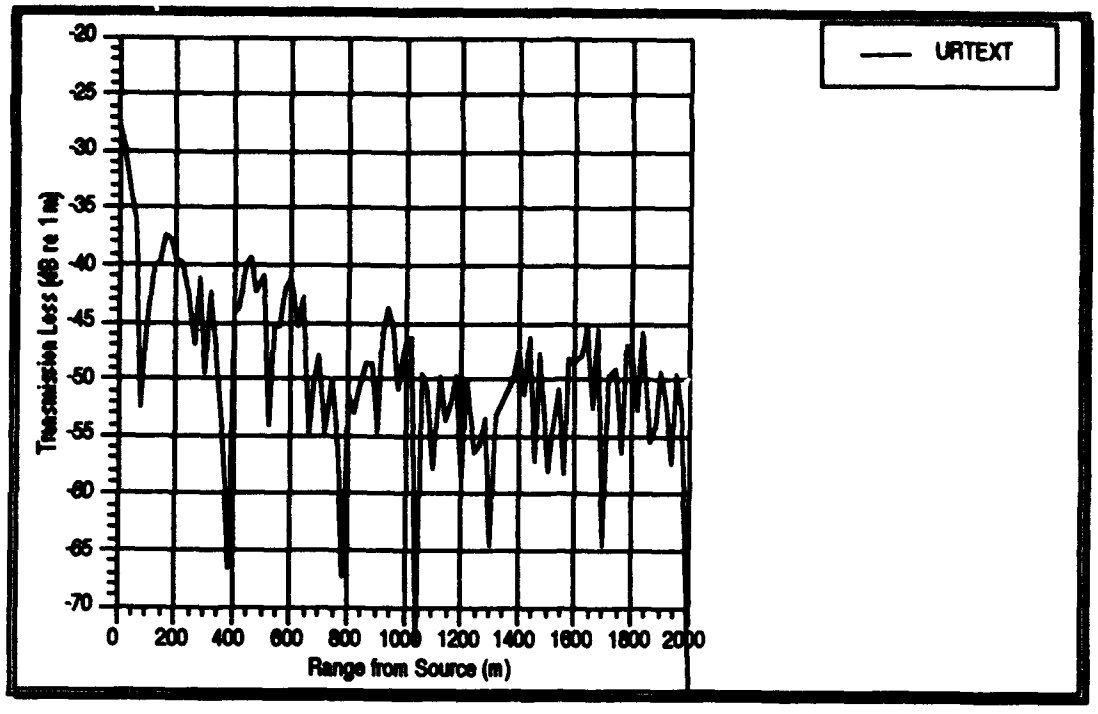

Figure 12 - Scenario 1 - 100 m Receiver Depth

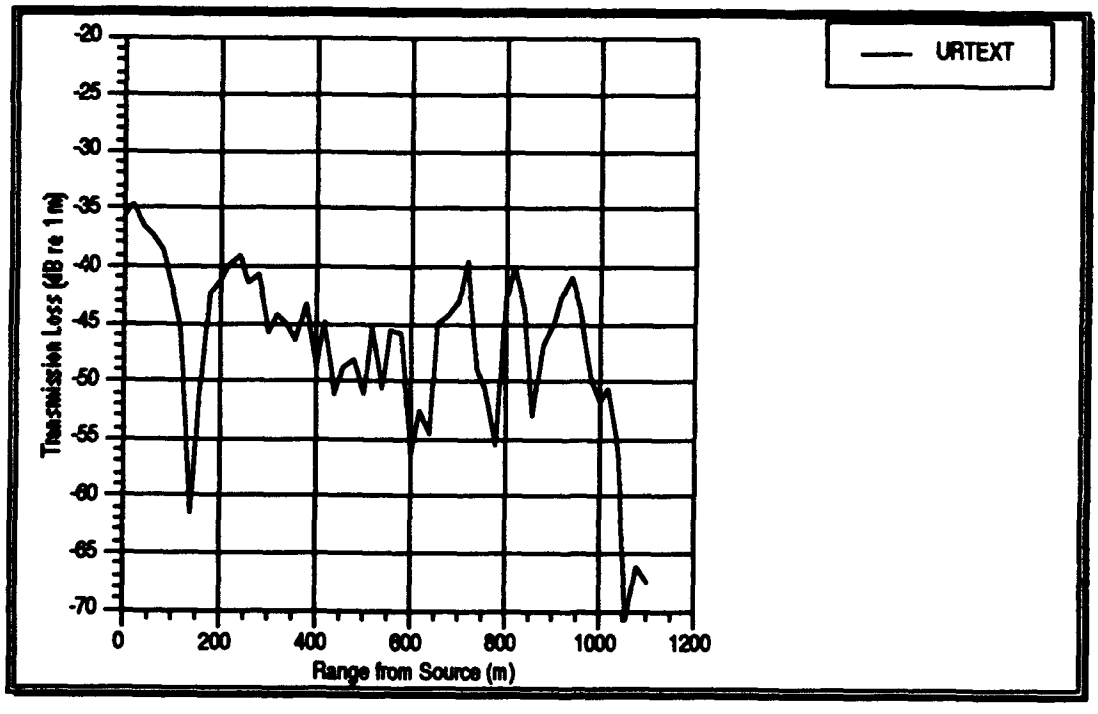

Figure 13 - Scenario 1 - 150 m Receiver Depth

C. SCENARIO TWO—FAST, LOSSLESS BOTTOM

In this scenario a more realistic environment was used. Inputs were as seen in Table 1. This produced the inputs for URTEXT as given in Table 2. Figures 14 through 17 are transmission loss profiles of both URTEXT and BBCM within the water column.

Only the water column is considered as URTEXT does not calculate pressures in the underlying bottom. However, areas of significant difference can be seen. These are primarily due to the effect of the rigid sub-bottom. Areas where BBCM show an increase in transmission loss are likely due to a normal mode going through transition, while areas where there is significant decrease in transmission loss are possibly due to modal interference.

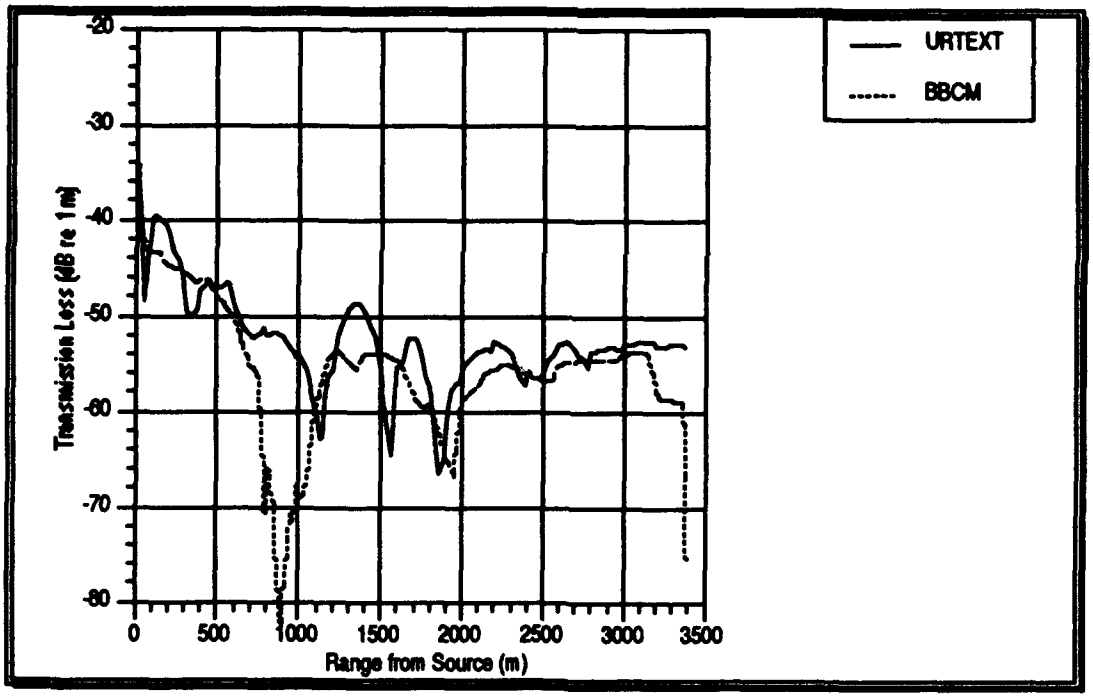

Figure 14 - Scenario 2 (Lossless Bottom) - 30 m Receiver Depth

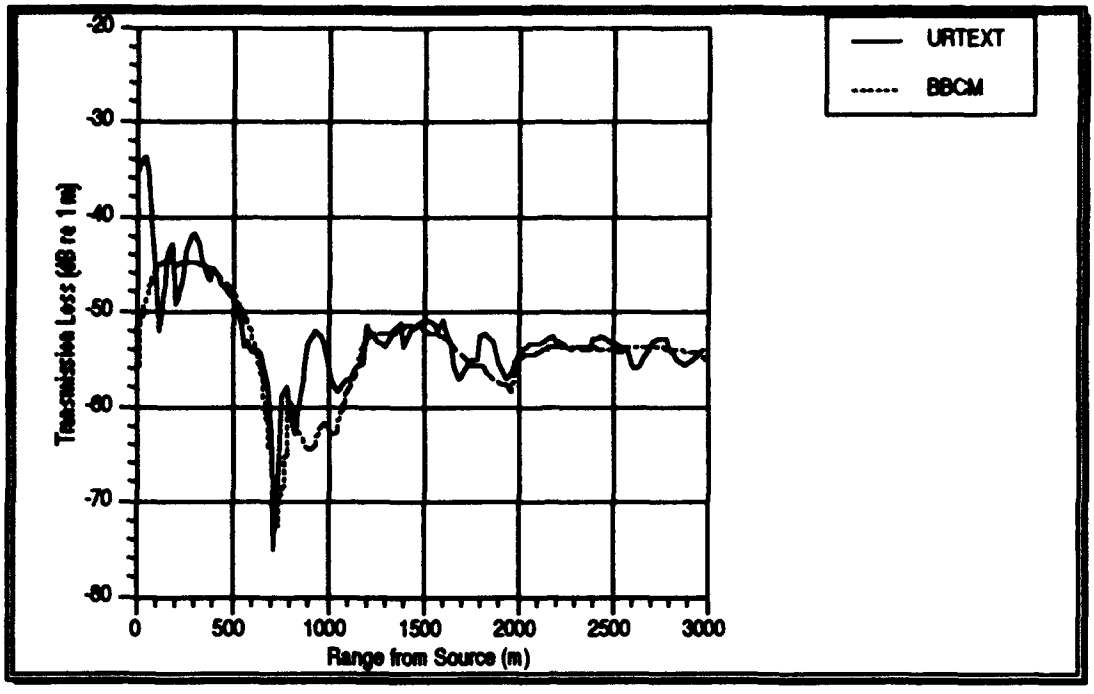

Figure 15 - Scenario 2 (Lossless Bottom) - 50 m Receiver Depth

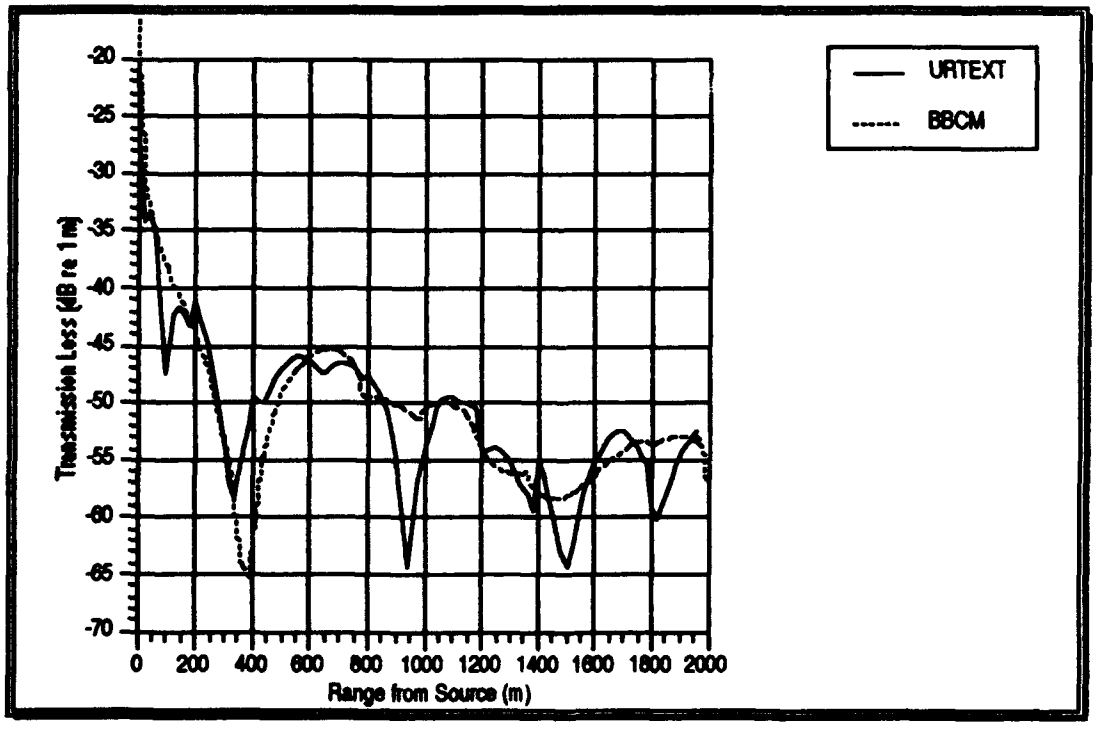

Figure 16 - Scenario 2 (Lossless Bottom) - 100 m Receiver Depth

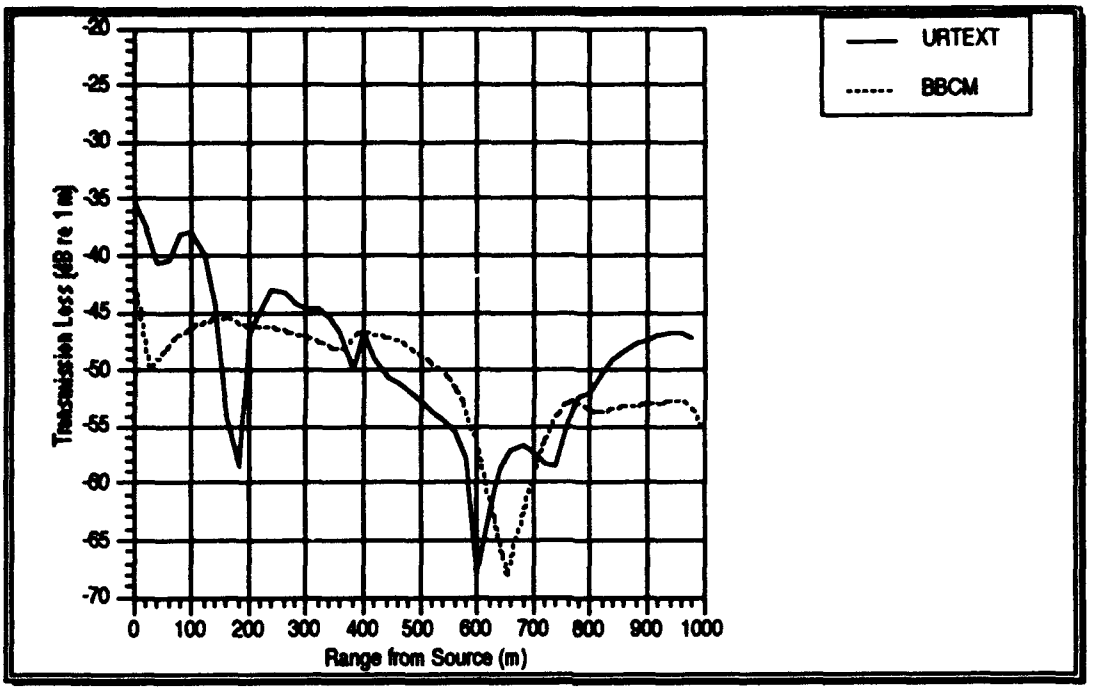

Figure 17 - Scenario 2 (Lossless Bottom) - 150 m Receiver Depth

D. SCENARIO 3—LOSSY BOTTOM

The environment for this run was the same as for Scenario 2, except a loss term of 0.5 dB/λ was added for the bottom. This converted to 0.07963 dB for the loss term in URTEXT. Figures 18 through 21 show the results of this run.

For this scenario, another difficulty was encountered. While the benchmark calls for attenuation by the bottom for the source frequency, that attenuation must be applied to the normal modes of interest. Therefore, a range dependent attenuation coefficient must be determined. Since no such coefficient can be applied, the results developed are rough approximations at best near or around modal cutoff.

BBCM runs were not accurate but are estimates. BBCM was run with three normal modes. Application of the attenuation term is a difficult exercise, first because it needs to be range dependent to more accurately eliminate the rigid sub-bottom, and second because the term must be distributed among the modes. Further research in this problem is necessary.

Again, good correlation is noted between the models. The addition of the attenuation term has no great effect on the sound in the water column. However, there is a significant drop-off at the end of the BBCM graphs. These are the points where the receivers are now in the bottom. Here the attenuation is significant.

Another significant feature is in Figure 18 at 150 m range. Here a dip is seen in URTEXT which is not seen in BBCM. At this relatively short range surface interference is noted. URTEXT picks this up (see Appendix A) but BBCM does not. Again, the original purpose of BBCM is to make predictions at relatively long ranges, significantly greater than the influence of surface interference [Ref 35]. At these longer ranges, BBCM is a robust model.

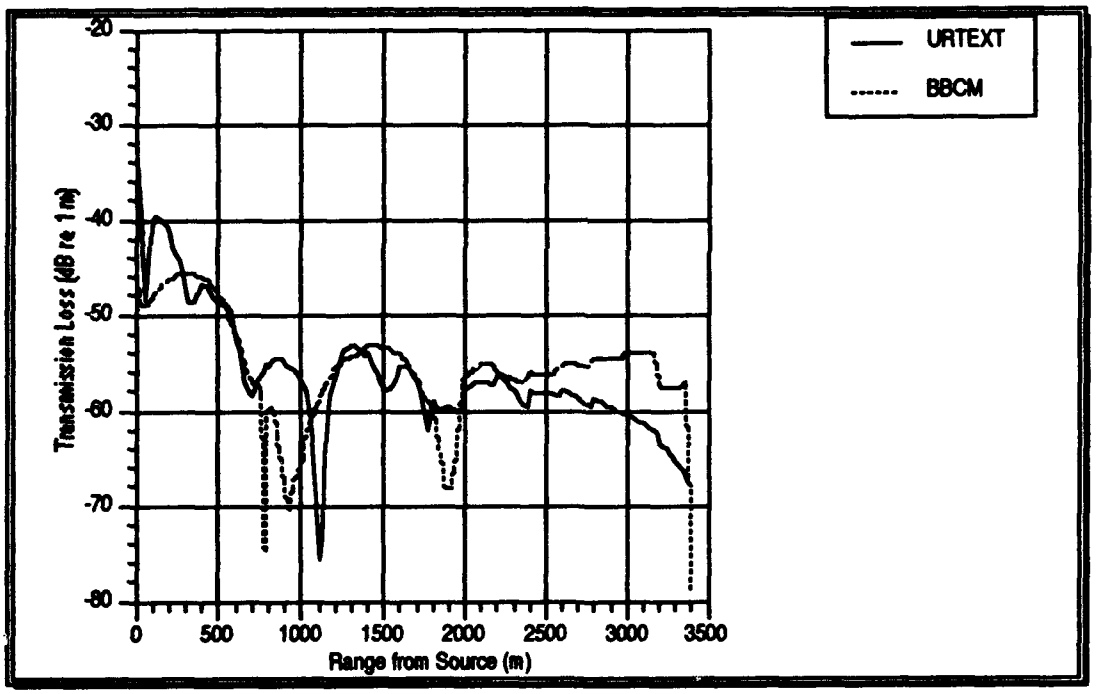

Figure 18 - Scenario 3 (Lossy Bottom) - 30 m Receiver Depth

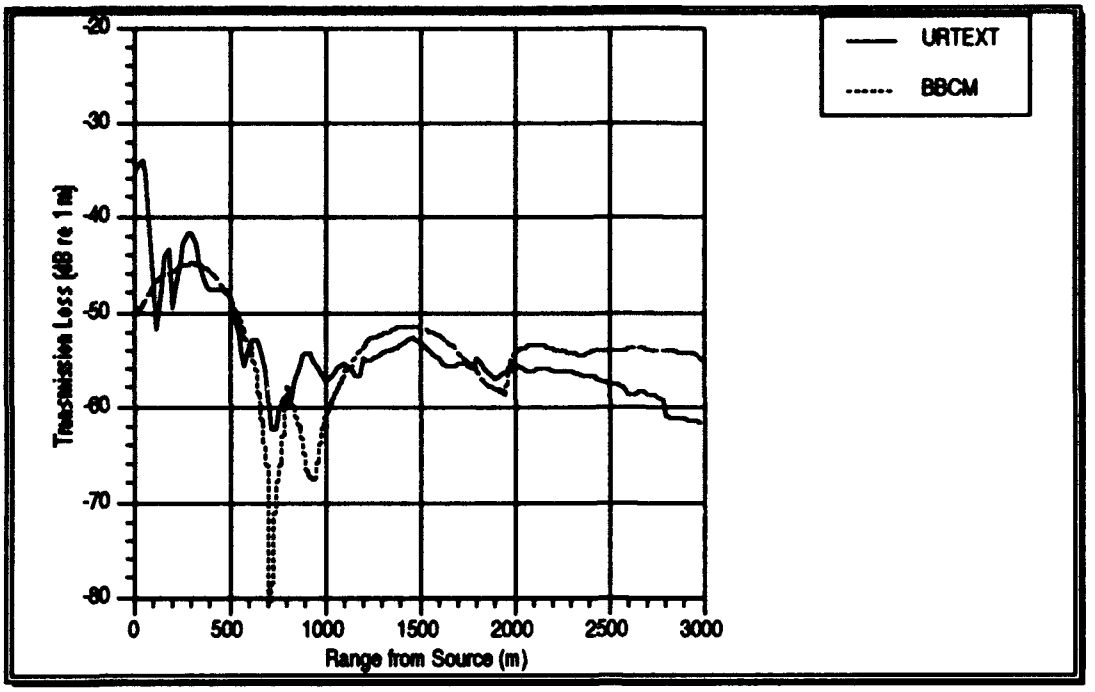

Figure 19 - Scenario 3 (Lossy Bottom) - 50 m Receiver Depth

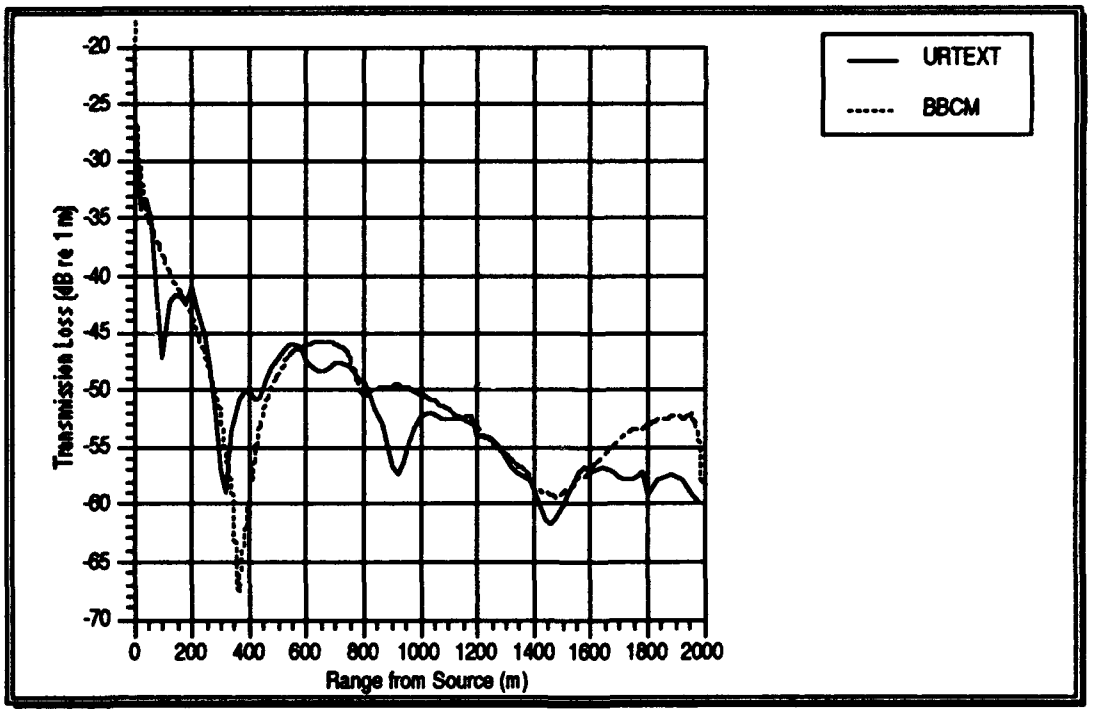

Figure 20 - Scenario 3 (Lossy Bottom) - 100 m Receiver Depth

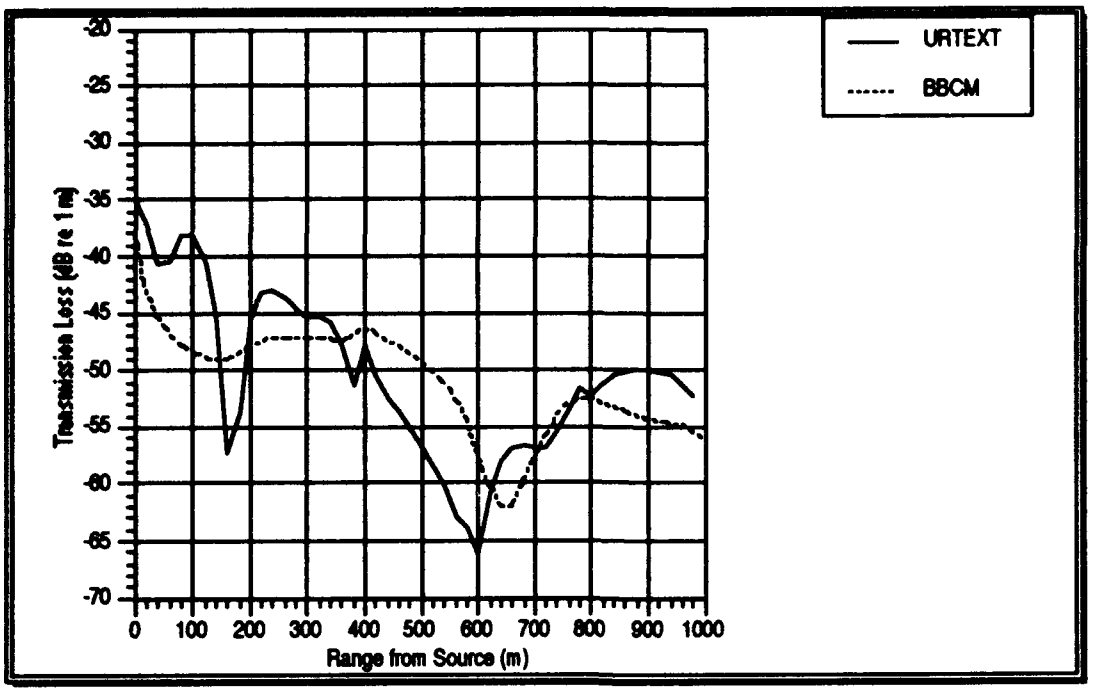

Figure 21 - Scenario 3 (Lossy Bottom) - 150 m Receiver Depth

IV. CONCLUSIONS AND RECOMMENDATIONS

Figures 22 through 25 show the results of Jensen and Ferla using a PE method compared to the results of URTEXT [Ref 36].

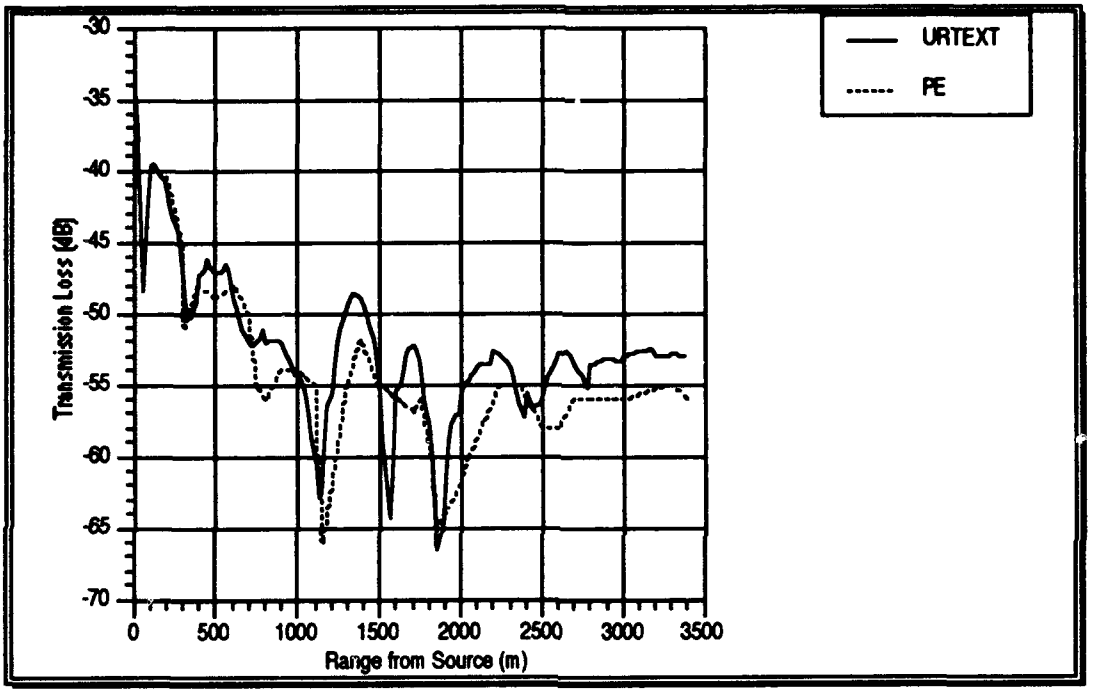

Figure 22 - Scenario 2 - 30 m comparison of PE and URTEXT

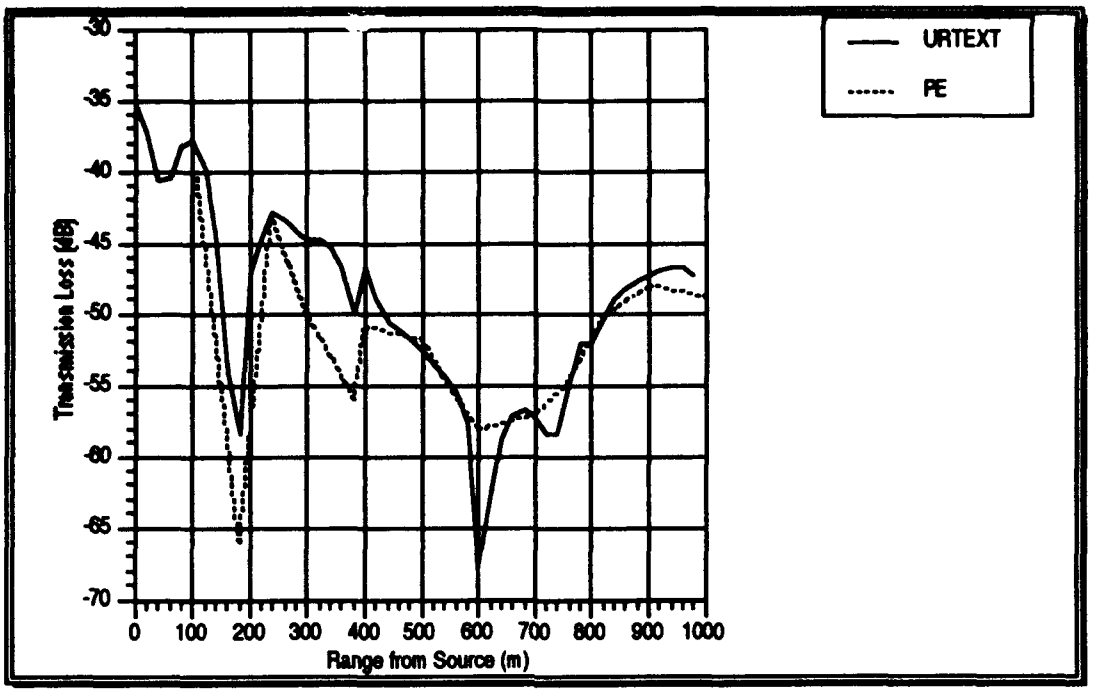

Figure 23 - Scenario 2 - 150 m Comparison of PE and URTEXT

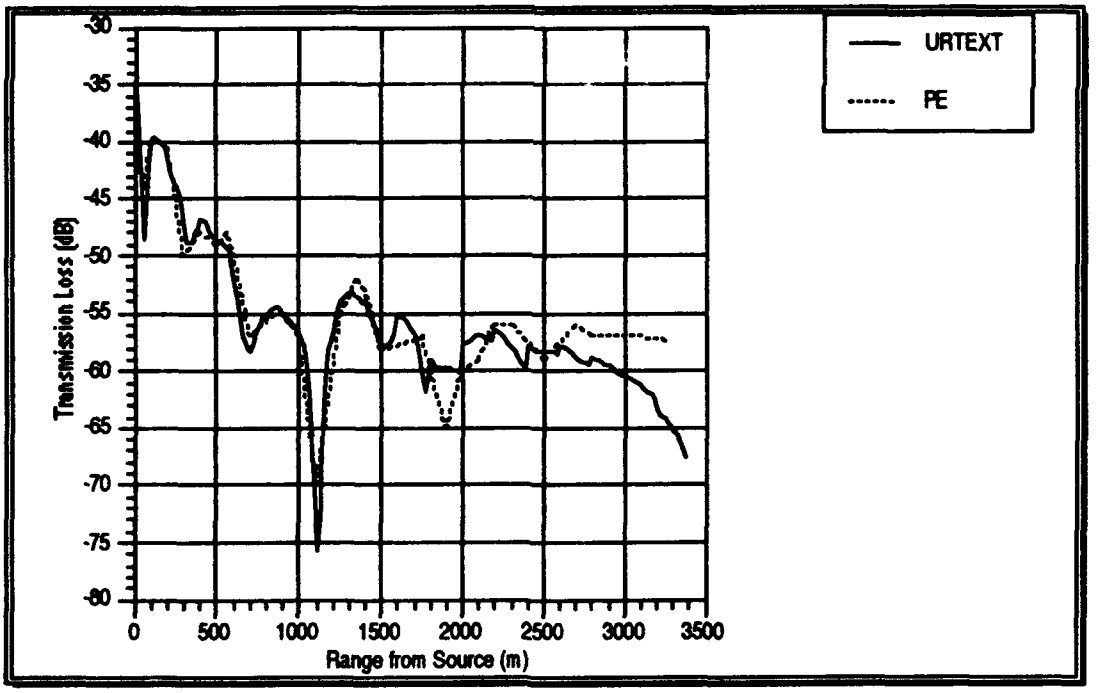

Figure 24 - Scenario 3 - 30 m Comparison of PE and URTEXT

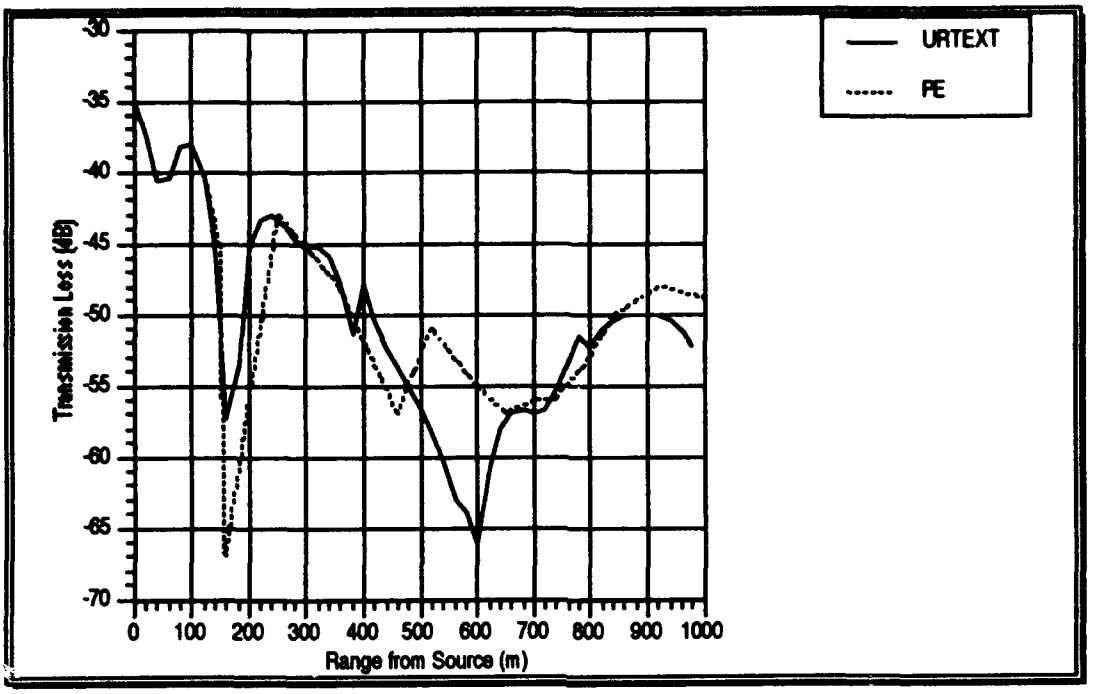

Figure 25 - Scenario 3 - 150 m Comparison of PE and URTEXT

For the cases examined—upslope propagation over both a lossless and lossy bottom, both URTEXT and BBCM have good agreement between the two. In the close range, BBCM does not show surface interference while URTEXT does. However, BBCM does develop a pressure field in the underlying bottom while URTEXT is effective only in the water column. Furthermore, BBCM is much quicker to create the pressure field. Using a range resolution of 25 m, BBCM created a pressure field for each scenario in 2.5 hours per run. Using the same equipment, URTEXT took 10 hours each run to develop the same resolution without calculating transmission loss in the bottom. BBCM therefore is more time effective.

Other strengths of BBCM are its flexibility. Because the input files model of the environment, different conditions can be simulated by changing the input files. Upslope, downslope, cross-canyon, stratified water or bottom layers can all be simulated. URTEXT is

limited only to the condition of the wedge shaped bottom. It is still a good tool for analysis of the specific problem, but BBCM is a more flexible tool for real world conditions.

Areas of further research present themselves. URTEXT needs to be sped up. MATLAB is very fast with matrix arithmetic and manipulation. A revision of URTEXT which takes advantage of this capability would be handy in the analysis of the wedge problem. Also, new developments to the image problem include using doublets and sets of four images. Perhaps including these as subroutines would speed up URTEXT.

The examination of a sloping interface over a rigid sub-bottom needs to be investigated. A modification of URTEXT to include this condition promises interesting results. Furthermore, a solution of the above problem which take incident angle needs to be determined.

Finally, both the downslope and cross-slope cases need to be investigated with BBCM. The upslope case is a standard comparison with other models, but predictions in either conditions might prove useful.

APPENDIX A

To develop a comparison standard between the image model and the coupled mode model, we translated the image program URTEXT from FORTRAN to MATLAB™ [Ref 37]. MATLAB is a high level scripting language which runs on a variety of computer operating systems including VAX, MS-DOS, UNIX, and Macintosh. This improved the flexibility of the image model to let it be run on desktop computers and advanced workstations. Furthermore, since the coupled mode model is also written in MATLAB, comparison of CPU run times can be made.

Validation of the MATLAB version of URTEXT, called URTEXTBAT, was conducted by comparing the results of URTEXTBAT to those of URTEXT as run on the IBM 3033 located at the Naval Postgraduate School. Table A-1 shows the input conditions of the programs. Pressure amplitudes were computed for scaling distances from three to ten dump distances from the wedge apex and at receiver angles from the surface to the bottom.

TABLE A-1

β	10°
γ	5°
r_1	2
ρ_1/ρ_2	2.0
c_1/c_2	0.5
α/k_2	0.001
y_0	0.0

Tables A-2, A-3, and A-4 show the results of the comparison. The major error at the surface is due to the difference in precision of the different languages. FORTRAN uses single precision variables, accurate to six decimal places. MATLAB is precise to 13 places,

therefore at the small pressures near the surface the round-off errors are extreme. Excluding the errors at the boundaries, the average absolute difference of the field was 0.00206.

TABLE A-2

FORTRAN	r_2							
δ	3	4	5	6	7	8	9	10
10	0.00324	0.00813	0.0026	0.00158	0.00118	0.00118	0.00153	0.0031
9	1.1393	0.75924	0.63381	0.4346	0.30078	0.2086	0.13697	0.0337
8	2.13245	1.17088	1.16923	0.80956	0.56091	0.38328	0.20159	0.14456
7	2.86145	1.4393	1.52998	1.07776	0.74823	0.47362	0.34154	0.34534
6	3.24737	1.6604	1.66464	1.20835	0.84126	0.5739	0.56706	0.5354
5	3.26776	1.93661	1.56257	1.19399	0.8313	0.79333	0.74299	0.67374
4	2.97124	2.06111	1.25278	1.05485	0.91045	0.9172	0.82486	0.72998
3	2.51693	1.97233	0.80655	0.84476	0.98048	0.90308	0.79069	0.68846
2	2.39419	1.65642	0.51872	0.72407	0.84396	0.74538	0.64007	0.55031
1	1.65191	1.13991	0.3643	0.54176	0.54487	0.46663	0.39299	0.33296
0	0.75925	0.48278	0.14244	0.15337	0.14283	0.11185	0.08627	0.06728

TABLE A-3

MATLAB™	r_2							
δ	3	4	5	6	7	8	9	10
10	0.0003	0.0008	0.0003	0.0002	0.0001	0.0001	0.0002	0.0003
9	1.1378	0.7536	0.6319	0.4337	0.3004	0.2087	0.1377	0.0358
8	2.1323	1.1668	1.1681	0.8093	0.5612	0.3845	0.2038	0.1422
7	2.8627	1.4368	1.5293	1.0781	0.7494	0.4822	0.3388	0.343
6	3.25	1.6586	1.6652	1.2094	0.8436	0.571	0.5643	0.5336
5	3.2716	1.9359	1.5637	1.1955	0.8286	0.7897	0.7412	0.6726
4	2.9753	2.0614	1.2543	1.0564	0.9016	0.9152	0.824	0.7296
3	2.5161	1.9736	0.8081	0.8451	0.9778	0.9026	0.7908	0.6887
2	2.3904	1.6583	0.5202	0.721	0.8439	0.746	0.6408	0.551
1	1.6515	1.1421	0.3659	0.5405	0.5463	0.468	0.3941	0.3339
0	0.7354	0.485	0.1428	0.1557	0.1449	0.1134	0.0875	0.0683

TABLE A-4

Absolute Difference	r_2							
δ	3	4	5	6	7	8	9	10
10	0.00294	0.00733	0.00230	0.00138	0.00108	0.00108	0.00133	0.00280
9	0.00150	0.00564	0.00191	0.00090	0.00038	0.00010	0.00073	0.00210
8	0.00015	0.00408	0.00113	0.00026	0.00029	0.00122	0.00221	0.00236
7	0.00125	0.00250	0.00068	0.00034	0.00117	0.00858	0.00274	0.00234
6	0.00263	0.00180	0.00056	0.00105	0.00234	0.00290	0.00276	0.00180
5	0.00384	0.00071	0.00113	0.00151	0.00270	0.00363	0.00179	0.00114
4	0.00406	0.00029	0.00152	0.00155	0.00885	0.00200	0.00086	0.00038
3	0.00083	0.00127	0.00155	0.00034	0.00268	0.00048	0.00011	0.00024
2	0.00379	0.00188	0.00148	0.00307	0.00006	0.00062	0.00073	0.00069
1	0.00041	0.00219	0.00160	0.00126	0.00143	0.00137	0.00111	0.00094
0	0.02385	0.00222	0.00036	0.00233	0.00207	0.00155	0.00123	0.00102

To see if the MATLAB is more precise, a run was made on an 18° slope with the data taken from the surface to 2° below sampled every 0.1°. Figure A-1 shows pressure falls off linearly as the sound nears the surface. This implies the model is valid at the boundaries.

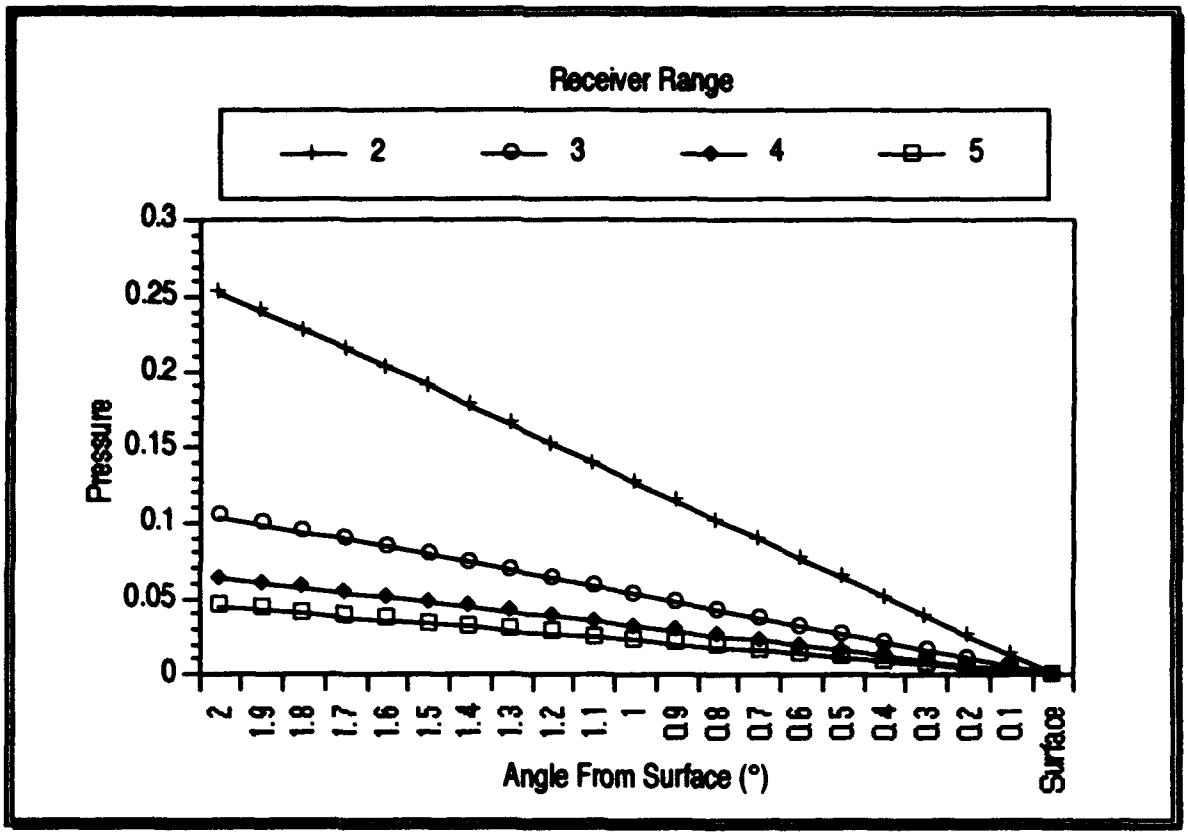

Figure A-1 - Boundary Condition Check

To further explore the differences between the two models, a third model, called WEDGESLO was used. This model was validated by Kaswandi [Ref 14]. This program is written in BASIC to be run on an MS-DOS based computer, but used double precision variables. A single run at r_2=5 showed correlation between WEDGESLO and URTEXTBAT to four places, including at the boundary.

Some special cases were run on URTEXTBAT before it was considered valid. First, to verify reciprocity of the field, the source was set at r_1=10 and γ varied from 0° to 10°. The receiver was fixed at δ = 5° and at r_2=2. Table A-5 shows the results and an error comparison. The errors are within the round off tolerance of the program, showing URTEXT as valid for both the upslope and downslope fields as well as validating the acoustic reciprocity of the model.

TABLE A-5 - RECIPROCITY CHECK

δ	Pressure	Difference
10	0	0.00310
9	0.03349	0.00021
8	0.14344	0.00112
7	0.34385	0.00149
6	0.53402	0.00138
5	0.67274	0.00100
4	0.72949	0.00049
3	0.6885	0.00004
2	0.55086	0.00055
1	0.33387	0.00091
0	0.06837	0.00109

Another test was run using matched acoustic impedance of the water and the bottom. The bottom then becomes transparent and the pressure field will be that of a surface interference effect (Lloyd's Mirror). Density and speed of sound ratios were set to .9999 and slope angle was set to 18°. The receiver was set at the same depth as the source and moved downslope. The pressure field predicted is approximated by the equation

$$P(r,h) = \frac{2A}{r}\left|\sin\frac{khd}{r}\right| \qquad \text{(A-1)}$$

where h and d are depths of the receiver and the source, A is the pressure amplitude at the source at one meter, and k is the wave number. Frequency used was 1000 Hz.

Figure A-2 shows a plot of pressure as a function of range from the source. Interference maxima and minima from URTEXTBAT match those predicted by equation (A-1).

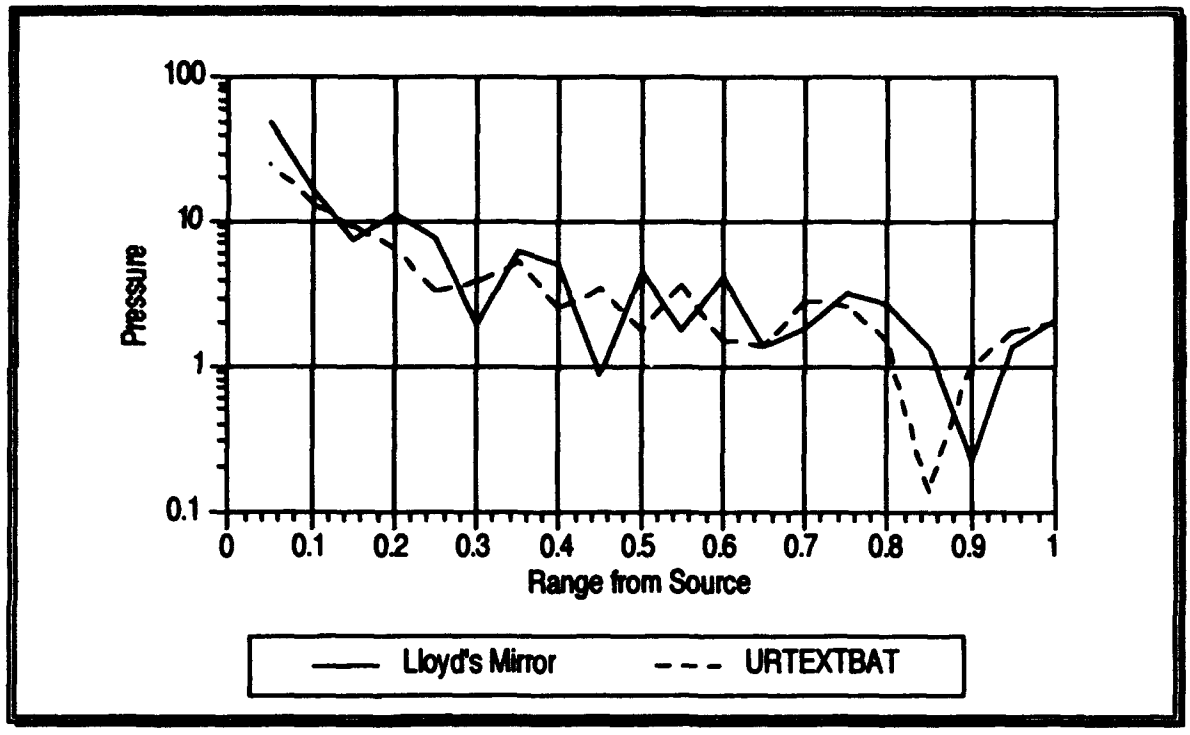

Figure A-2a - Close Range Surface Interferance

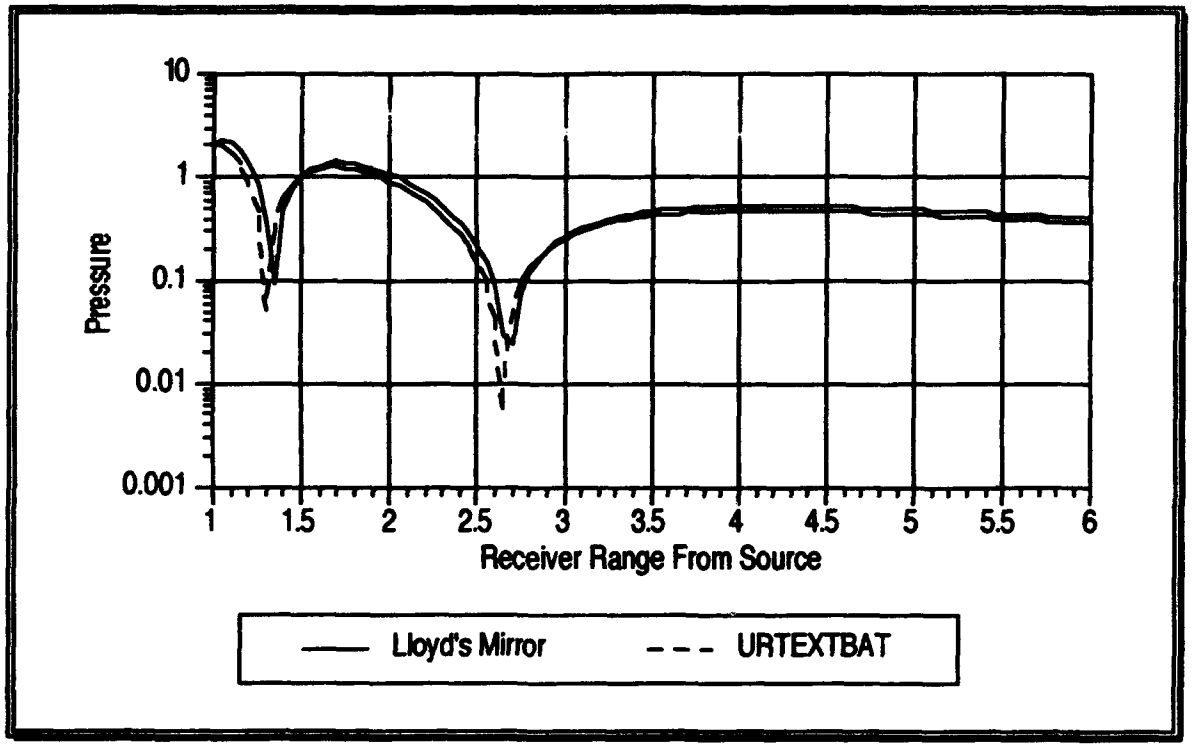

Figure A-2b - Long Range Surface Interferance

As seen from the above, URTEXTBAT has undergone extensive proofing. When compared with previous versions in FORTRAN and BASIC, it is more flexible both in platforms run and model variables. While the program does not take full advantage of the features of MATLAB, and has significant room for optimizations, the program in its present form is more than sufficient for the purposes of this research.

APPENDIX B

```
%%%%%%%%%%%%%%%%%%%%%%%%
%
%  URTEXT for MATLAB
%
%  Adapted from FORTRAN
%
%%%%%%%%%%%%%%%%%%%%%%%%
%%%%%%%%%%%%%%%%%%%%%%%%
% Enter Input Variables
% Required are: Range of Source and Receiver
% Wedge angle in Degrees
% Source and Reciever angles from the Bottom
% Speed of sound ratio and density ratios
% Bottom loss coefficient and cross slope range
%%%%%%%%%%%%%%%%%%%%%%%%

B=input('Enter bottom wedge angle: ');
G=input('Enter source angle from the surface: ');
D=input('Enter receiver angle from the surface: ');
rho1=input('Enter Density ratio, water to bottom: ');
CC=input('Enter speed ratio, water to bottom: ');
r1=input('Enter range of source from apex: ');
r2=input('Enter range of receiver from apex: ');
AL=input('Enter bottom loss coefficient: ');
y0=input('Enter cross-slope range: ');

% Determine number of image pairs
% and convert to radians. Also determine constants

% Function rads(A) converts degrees into radians
% Contained as a seperate M-File in the MATLAB Toolbox

function X=rads(A)
% Converts degrees into radians
X=A*pi/180;
end


N1=fix(180/B);
B=rads(B);
G=rads(G);
D=rads(D);
c2=CC^2;

%%%%%%%%%%%%%%%%%%%%%%%%
% Determine scaling for fast or slow bottom
%%%%%%%%%%%%%%%%%%%%%%%%

tqq=tan(B);
if CC<1,
   tqq1=acos(CC);
   tqq2=sin(tqq1);
else
   tqq1=acos(1/CC);
   tqq2=tan(tqq1);
end;
```

```
tqq3=2*tqq2*tqq;
t4=pi/tqq3;
q1=1/sqrt(2);
d2=r1^2+r2^2+y0^2;
r3=2*r1*r2;
s1=1;

%%%%%%%%%%%%%%%%%%%%%%%%
% Determine range to receiver for each image
%%%%%%%%%%%%%%%%%%%%%%%%

for n=1:1:N1,
   if s1>0
      t1(n)=(n-1)*B+G;
   else
      t1(n)=n*B-G;
   end;
   s1=-s1;
   r8(n)=sqrt(d2-r3*cos(t1(n)-D));
   r9(n)=sqrt(d2-r3*cos(t1(n)+D));
end;
p1=0;p2=0;
for n=1:1:N1,
   s2=(-1)^(fix(n/2));

%%%%%%%%%%%%%%%%%%%%%%%%
% Calculate Reflection Coefficient for Upper Space
%%%%%%%%%%%%%%%%%%%%%%%%

   w1=2*c2*AL;
   i1=fix((n-1)/2);
   for i=1:1:i1,
      s(i)=abs(r1*sin(t1(n)-2*i*B)+r2*sin(2*i*B-D))/r8(n);
      if s(i)>=1,
         s(i)=1;
      end;
      c(i)=sqrt(1-(s(i)^2));
      t=s(i)/rho1;
      w0=(-c2+(c(i)^2));
      y=sqrt((w0^2)+(w1^2));
      z=abs(w0);
      if y<=z,
         y=z;
      end;
      y1=q1*sqrt(y+w0);
      y2=-q1*sqrt(y-w0);
      z1=t-y2;
      z2=-y1;
      z3=z1/(z1^2+z2^2);
      z4=-z2/(z1^2+z2^2);
      z1=t+y2;
      z2=y1;
      z5=z1*z3-z2*z4;
      z6=z1*z4+z2*z3;
      e(i)=z5;
      f(i)=z6;
   end;

%%%%%%%%%%%%%%%%%%%%%%%%
% Determine Pressure Contribution for each upper image
%%%%%%%%%%%%%%%%%%%%%%%%
```

```
   z1=0;z2=0;z3=0;z4=0;z5=1;z6=0;
   if n>2,
      for i=1:1:i1,
         z1=e(i);
         z2=f(i);
         z3=z5;
         z4=z6;
         z5=z1*z3-z2*z4;
         z6=z1*z4+z2*z3;
      end;
   end;
   z1=z5;
   z2=z6;
   t=t4*r8(n);
   z3=cos(t);
   z4=-sin(t);
   z5=z1*z3-z2*z4;
   z6=z1*z4+z2*z3;
   p1=p1+s2*z5/r8(n);
   p2=p2+s2*z6/r8(n);
   i1=i1+1;

%%%%%%%%%%%%%%%%%%%%%%%%
% Determine Reflection Coefficient for the Lower Images
%%%%%%%%%%%%%%%%%%%%%%%%

   for i=1:1:i1,
      s(i)=abs(r1*sin(t1(n)-2*(i-1)*B)+r2*sin(2*(i-1)*B+D))/r9(n);
      if s(i)>1,
         s(i)=1;
      end;
      c(i)=sqrt(1.0001-s(i)^2);
      t=s(i)/rho1;
      w0=-c2+c(i)^2;
      y=sqrt(w0^2+w1^2);
      z=abs(w0);
      if y<=z,
         y=z;
      end;
      y1=q1*sqrt(y+w0);
      y2=-q1*sqrt(y-w0);
      z1=t-y2;
      z2=-y1;
      z3=z1/(z1^2+z2^2);
      z4=-z2/(z1^2+z2^2);
      z1=t+y2;
      z2=y1;
      z5=z1*z3-z2*z4;
      z6=z1*z4+z2*z3;
      e(i)=z5;
      f(i)=z6;
   end;

%%%%%%%%%%%%%%%%%%%%%%%%
% Find Pressure Contribution for Lower Images
%%%%%%%%%%%%%%%%%%%%%%%%

   z1=0;z2=0;z3=0;z4=0;z5=1;z6=0;
   for i=1:1:i1,
      z1=e(i);
```

```
        z2=f(i);
        z3=z5;
        z4=z6;
        z5=z1*z3-z2*z4;
        z6=z1*z4+z2*z3;
    end;
    z1=z5;
    z2=z6;
    t=t4*r9(n);
    z3=cos(t);
    z4=-sin(t);
    z5=z1*z3-z2*z4;
    z6=z1*z4+z2*z3;
    p1=p1+s2*z5/r9(n);
    p2=p2+s2*z6/r9(n);
end;

%%%%%%%%%%%%%%%%%%%%%%%%
% Total Pressure at the reciever is:
%%%%%%%%%%%%%%%%%%%%%%%%

pz=sqrt(p1^2+p2^2);
end;
```

```
%%%%%%%%%%%%%%%%%%%%%%%%
%
%    URTEXTBAT for MATLAB
%
%    Adapted from FORTRAN
%
%%%%%%%%%%%%%%%%%%%%%%%%
% This program determines a 2 dimensional
% Sound pressure field over a sloping bottom
%%%%%%%%%%%%%%%%%%%%%%%%
% Enter Input Variables
% Required are: Range of Source
% Maximum range of the Receiver
% Wedge angle in Degrees
% Source angle from the Surface
% Speed of sound ratio and density ratios
% Bottom loss coefficient and cross slope range.
% The program determines receiver angles over 10 increments
% and range from source range + one dump distance to the
% maximum receiver range
%%%%%%%%%%%%%%%%%%%%%%%%

B=input('Enter bottom wedge angle: ');
G=input('Enter source angle from the surface: ');
rho1=input('Enter Density ratio, water to bottom: ');
CC=input('Enter speed ratio, water to bottom: ');
r1=input('Enter range of source from apex: ');
range=input('Enter maximum receiver range: ');
AL=input('Enter bottom loss coefficient: ');
b=B/10;countk=0;countl=0;
y0=input('Enter cross slope range: ');

%%%%%%%%%%%%%%%%%%%%%%%%
% Determine number of image pairs
% and convert angles to radians
%%%%%%%%%%%%%%%%%%%%%%%%

time=clock;
N1=fix(180/B);
B=rads(B);
G=rads(G);

%%%%%%%%%%%%%%%%%%%%%%%%
% Loop for field calculation
%%%%%%%%%%%%%%%%%%%%%%%%

for k=r1+1:range/10:range,
   r2=k;
   countk=countk+1;
   for l=0:b:b*10,
      D=1;countl=countl+1;
      D=rads(D);
      c2=CC^2;

%%%%%%%%%%%%%%%%%%%%%%%%
% Find scaling distance for fast or slow bottom
%%%%%%%%%%%%%%%%%%%%%%%%

      tqq=tan(B);
      if CC<1,
```

```
         tqq1=acos(CC);
         tqq2=sin(tqq1);
      else
         tqq1=acos(1/CC);
         tqq2=tan(tqq1);
      end;
      tqq3=2*tqq2*tqq;
      t4=pi/tqq3;
      q1=1/sqrt(2);
      d2=r1^2+r2^2+y0^2;
      r3=2*r1*r2;
      s1=1;

%%%%%%%%%%%%%%%%%%%%%%%%
% Determine range for each image to reciever
%%%%%%%%%%%%%%%%%%%%%%%%

      for n=1:1:N1,
         if s1>0
            t1(n)=(n-1)*B+G;
         else
            t1(n)=n*B-G;
         end;
         s1=-s1;
         r8(n)=sqrt(d2-r3*cos(t1(n)-D));
         r9(n)=sqrt(d2-r3*cos(t1(n)+D));
      end;
      p1=0;p2=0;
      for n=1:1:N1,

%%%%%%%%%%%%%%%%%%%%%%%%
% Find Reflection coefficient for upper images
%%%%%%%%%%%%%%%%%%%%%%%%

         s2=(-1)^(fix(n/2));
         w1=2*c2*AL;
         i1=fix((n-1)/2);
         for i=1:1:i1,
            s(i)=abs(r1*sin(t1(n)-2*i*B)+r2*sin(2*i*B-D))/r8(n);
            if s(i)>=1,
               s(i)=1;
            end;
            c(i)=sqrt(1-(s(i)^2));
            t=s(i)/rho1;
            w0=(-c2+(c(i)^2));
            y=sqrt((w0^2)+(w1^2));
            z=abs(w0);
            if y<=z,
               y=z;
            end;
            y1=q1*sqrt(y+w0);
            y2=-q1*sqrt(y-w0);
            z1=t-y2;
            z2=-y1;
            z3=z1/(z1^2+z2^2);
            z4=-z2/(z1^2+z2^2);
            z1=t+y2;
            z2=y1;
            z5=z1*z3-z2*z4;
            z6=z1*z4+z2*z3;
            e(i)=z5;
```

```
            f(i)=z6;
         end;
         z1=0;z2=0;z3=0;z4=0;z5=1;z6=0;
         if n>2,
            for i=1:1:i1,
               z1=e(i);
               z2=f(i);
               z3=z5;
               z4=z6;
               z5=z1*z3-z2*z4;
               z6=z1*z4+z2*z3;
            end;
         end;

%%%%%%%%%%%%%%%%%%%%%%%%
% Find Pressure contribution of upper images
%%%%%%%%%%%%%%%%%%%%%%%%

         z1=z5;
         z2=z6;
         t=t4*r8(n);
         z3=cos(t);
         z4=-sin(t);
         z5=z1*z3-z2*z4;
         z6=z1*z4+z2*z3;
         p1=p1+s2*z5/r8(n);
         p2=p2+s2*z6/r8(n);
         i1=i1+1;
         for i=1:1:i1,

%%%%%%%%%%%%%%%%%%%%%%%%
% Find refection coefficient for lower images
%%%%%%%%%%%%%%%%%%%%%%%%

            s(i)=abs(r1*sin(t1(n)-2*(i-1)*B)+r2*sin(2*(i-1)*B+D))/r9(n);
            if s(i)>1,
               s(i)=1;
            end;
            c(i)=sqrt(1.0001-s(i)^2);
            t=s(i)/rho1;
            w0=-c2+c(i)^2;
            y=sqrt(w0^2+w1^2);
            z=abs(w0);
            if y<=z,
               y=z;
            end;
            y1=q1*sqrt(y+w0);
            y2=-q1*sqrt(y-w0);
            z1=t-y2;
            z2=-y1;
            z3=z1/(z1^2+z2^2);
            z4=-z2/(z1^2+z2^2);
            z1=t+y2;
            z2=y1;
            z5=z1*z3-z2*z4;
            z6=z1*z4+z2*z3;
            e(i)=z5;
            f(i)=z6;
         end;
         z1=0;z2=0;z3=0;z4=0;z5=1;z6=0;
         for i=1:1:i1,
```

```
            z1=e(i);
            z2=f(i);
            z3=z5;
            z4=z6;
            z5=z1*z3-z2*z4;
            z6=z1*z4+z2*z3;
         end;

%%%%%%%%%%%%%%%%%%%%%%%%
% Find Pressure contribution for lower images
%%%%%%%%%%%%%%%%%%%%%%%%

         z1=z5;
         z2=z6;
         t=t4*r9(n);
         z3=cos(t);
         z4=-sin(t);
         z5=z1*z3-z2*z4;
         z6=z1*z4+z2*z3;
         p1=p1+s2*z5/r9(n);
         p2=p2+s2*z6/r9(n);
      end;

%%%%%%%%%%%%%%%%%%%%%%%%
% Total pressure at the reciever is:
%%%%%%%%%%%%%%%%%%%%%%%%

      pz(count1,countk)=sqrt(p1^2+p2^2);

%%%%%%%%%%%%%%%%%%%%%%%%
% Reset variables
%%%%%%%%%%%%%%%%%%%%%%%%

      clear c;clear c2;clear d2;clear e; clear f;clear i; clear i1;
      clear n;clear p1;clear p2;clear q1;clear r3;clear r8; clear r9;
      clear s;clear s1;clear s2;clear t;clear t1;
      clear tqq;clear tqq1;clear tqq2;clear tqq3;clear w0; clear w1;
      clear y;clear y1;clear y2;clear z;clear z1;clear z2; clear z3;
      clear z4;clear z5;clear z6;
      end;
   count1=0;
et=etime(clock,time)
end;
```

```
%%%%%%%%%%%%%%%%%%%%%%%%
%
% SCENEGEN.M
%
%%%%%%%%%%%%%%%%%%%%%%%%
%
% This program creates input files for BBCM,
% the coupled mode model by Dr. C.S. Chiu.
% This program creates the inputs for a wedge shaped
% ocean overlying a fluid bottom.
% Both water and bottom are considered uniform in characteristics
% in depth. No irregularities in the bottom depth are
% generated, nor stratifications in sound velocity profile.
%
%%%%%%%%%%%%%%%%%%%%%%%%

% Input all the pertinent data
B=input('Enter wedge angle: ');
B=rads(B);
z=input('Enter maximum depth of the water column: ');
w=input('Enter length of the waveguide: ');
dw=input('Enter range resolution: ');
dz=input('Enter depth resolution: ');
c1=input('What is the speed of sound in the water? ');
c2=input('What is the speed of sound in the bottom? ');
r1=input('What is the density of the water? ');
r2=input('What is the density of the bottom? ');
n=input('How many modes? ');
ak=input('What is the bottom loss coefficient?');
f=input('What is the source frequency? ');

% Build data files -- range
r=0:dw:w;
save r.dat r /ascii;

% receiver depth
zr=0:10:z;
save zr.dat zr /ascii;

% attenuation matrix
for i=1:1:n,
   attenu(n)=ak;
end;
save attenu.dat attenu /ascii;

% sound speed profile
a=w/dw; b=z/dz;
t=tan(B);
for i=1:1:a+1,
   for j=1:1:b+1,
      if t>(j-1)*dz/(w-(i-1)*dw),
         c(j,i)=c1;
      else
         c(j,i)=c2;
      end;
   end;
end;
dummy=c(1:b,:);
for i=1:1:b,
   dummy(i,1)=c2;
end;
```

```
for i=2:1:a,
   dummy(:,i)=dummy(:,i-1);
end;
c=[c;dummy;dummy;dummy;dummy;dummy;dummy;dummy;dummy;dummy];
save c.dat c /ascii;

% density profile
for i=1:1:a+1,
   for j=1:1:b+1,
      if t>(j-1)*dz/(w-(i-1)*dw),
         rho(j,i)=r1;
      else
         rho(j,i)=r2;
      end;
   end;
end;
dummy=rho(1:b,:);
for i=1:1:b,
   dummy(i,1)=r2;
end;
for i=2:1:a,
   dummy(:,i)=dummy(:,i-1);
end;
rho=[rho;dummy;dummy;dummy;dummy;dummy;dummy;dummy;dummy;dummy];
save rho.dat rho /ascii;

% Source Spectrum Density Profile
ssp=[0 0;f-0.005 1;f 1;f+0.005 1;1000 0];
save ssp.dat ssp /ascii;
```

LIST OF REFERENCES

1. Tappert, F. D., "The Parabolic Approximation Method", *Wave Propagation and Underwater Acoustics*, J. B. Keller and J. S. Papadakis, eds., Springer 1977.

2. Collins, M. D., "Application and Time-domain Solution of Higher-Order Parabolic Equation in Underwater Acoustics", *J. Acoust. Soc. Am.*, **86**(3), September 1989.

3. Jensen, F. B. and Kuperman, W. A., "Sound Propagation in a Wedge-Shaped Ocean with a Penetrable Bottom", *J. Acoust. Soc. Am.*, **67**(5), May 1980.

4. Coppens, A. B. and Sanders, J. V., "Transmission of Sound into a Fast Fluid Bottom from an Overlying Fluid Wedge", *Proceedings of Workshop on Seismic Propagation in Shallow Water*, Office of Naval Research, Arlington, Virginia, 1978.

5. Jensen, F. B. and Tindle, C. T., "Numerical Modeling Results for Mode Propagation in a Wedge", *J. Acoust. Soc. Am.*, **82**(1), July 1987.

6. Lee, D. and McDaniel, S. T., "A Finite-Difference Treatment of Interface Conditions for the Parabolic Wave Equation: The Irregular Interface", *J. Acoust. Soc. Am.*, **73**(5), May 1983.

7. Collins, M. D., "The Rotated Parabolic Equation and Sloping Ocean Bottoms", *J. Acoust. Soc. Am.*, **87**(3), March 1990.

8. Fawcett, J. A., "Modeling Three-Dimensional Propagation in an Oceanic Wedge Using Parabolic Equation Methods", *J. Acoust. Soc. Am.*, **93**(5), May, 1993.

9. Macpherson, J. D. and Daintith, M. J., "Practical Model of Shallow Water Acoustic Propagation", *J. Acoust. Soc. Am.*, **41**(4), 1966.

10. Coppens, A. B., Sanders, J. V., Ioannou, G. I., and Kawamura, M., *Two Computer Programs for the Evaluation of the Acoustic Pressure Amplitude and Phase at the Bottom of a Wedge Shaped, Fluid Layer Overlying a Fast, Fluid Half Space*; Technical Report #NPS-61-79-002, Naval Postgraduate School, Monterey, CA, December 1978.

11. Brekhovskikh, L. and Lysanov, Yu., *Fundamentals of Ocean Acoustics*, Springer-Verlag, Berlin Heidelberg New York; 1982.

12. Baek, C., *The Acoustic Pressure in a Wedge-Shaped Water Layer Overlying a Fast Fluid Bottom*, Master's Thesis, Naval Postgraduate School, Monterey, CA, March 1984.

13. LeSesne, P. K., *Development of Computer Programs Using the Method of Images to Predict the Sound Field in a Wedge Overlaying a Fast Fluid and Comparison with Laboratory Experiments*, Master's Thesis, Naval Postgraduate School, Monterey, CA December 1984.

14. Kaswandi, C., *A Computerized Investigation Using the Method of Images to Predict the Sound Field in a Fluid Wedge Overlying a Slow Half-Space*, Master's Thesis, Naval Postgraduate School, Monterey, CA, December 1987.

15. Li Yu-Ming, *Acoustic Pressure Distribution on the Bottom of a Wedge Shaped Ocean*, Master's Thesis, Naval Postgraduate School, Monterey, CA, December 1987.

16. Nassopoulos, G., *Study of Sound Propagation in a Wedge Shaped Ocean and Comparison with Other Methods*, Master's Thesis, Naval Postgraduate School, Monterey, CA June 1992.

17. Deane, G. B. and Buckingham, M. J., "An Analysis of the Three-Dimensional Sound Field in a Penetrable Wedge with a Stratified Fluid or Elastic Basement", *J. Acoust. Soc. Am.*, **93**(3), March 1993.

18. Livingood, D. M., *Extension of the Analytical Approximation to the Transmission of Sound in Shallow Water Using the Image Model*, Master's Thesis, Naval Postgraduate School, Monterey, CA, September 1992.

19. Joyce, M. D., *Quadruplet Expansion of the Acoustic Pressure Field in a Wedge Shaped Ocean*, Master's Thesis, Naval Postgraduate School, Monterey, CA, September 1993.

20. Kim Jong Rok, *Comparison of Sound Pressure in a Wedge Shaped Ocean as Predicted by an Image Method and a PE Model*, Master's Thesis, Naval Postgraduate School, Monterey, CA December 1990.

21. Jaeger, L. E., *A Computer Program for Solving the Parabolic Equation Using an Implicit Finite-Difference Solution Method Incorporating Exact Interface Conditions*, Master's Thesis, Naval Postgraduate School, Monterey, California, September 1983.

22. Pierce, A. D., "Extension of the Method of Normal Modes to Sound Propagation in an Almost-Stratified Medium", *J. Acoust. Soc. Am.*, **36**(1), January 1965.

23. Graves, R. D., Nagl, A., Uberall, H., and Zarur, G. L., "Range-Dependent Normal Modes in Underwater Sound Propagation: Application to the Wedge Shaped Ocean", *J. Acoust. Soc. Am.*, **58**(6), December 1975.

24. Bradley, D., and Hudimac, A. A., *The Propagation of Sound in a Wedge Slow Duct*, Master's Thesis, The Catholic University of America, Washington D.C., 1970.

25. Buckingham, M. J., "Theory of Three-Dimensional Acoustic Propagation in a Wedgelike Ocean with a Penetrable Bottom", *J. Acoust. Soc. Am.*, **82**(1), July 1987.

26. Pierce, A. D., "Augmented Adiabatic Mode Theory for Upslope Propagation from a Point Source in a Variable-Depth Shallow Water Overlying a Fluid Bottom", *J. Acoust. Soc. Am.*, **74**(6), December 1983.

27. Arnold, J. M. and Felsen, L. B., "Rays and Local Modes in a Wedge-Shaped Ocean", *J. Acoust. Soc. Am.*, **73**(4), April 1983.

28. Arnold, J. M. and Felsen, L. B. "Intrinsic Modes in a Nonseparable Ocean Waveguide", *J. Acoust. Soc. Am.*, **76**(3), September 1984.

29. Avudainayagam, K. V. and Anand, G. V., "Application of Ray Theory with Beam Displacement to Three-dimensional Sound Propagation in a Wedge-Shaped Ocean", *J. Acoust. Soc. Am.*, **93**(5), May 1993.

30. Evans, R. B., "A Coupled Mode Solution for Acoustic Propagation in a Waveguide with Stepwise Depth Variation of a Penetrable Bottom", *J. Acoust. Soc. Am.*, **74**(1), July 1983.

31. Desaubies, Y., Chiu, C. S., and Miller, J., "Acoustic Mode Propagation in a Range-Dependent Ocean", *J. Acoust. Soc. Am*, **80**(4), 1986.

32. Chiu, C. S., and Ehret, L. L., "Computation of Sound Propagation in a Three-Dimensionally Varying Ocean: A Coupled Normal Mode Approach", *Computational Acoustics II*, Elsevier Science Publishers B. V., 1990.

33. Sagos, G. A., *A Three-Dimensional Coupled Normal Mode Model for Sound Propagation in Shallow Water with Irregular Bottom Bathymetry*, Master's Thesis, Naval Postgraduate School, Monterey, CA, December 1992.

34. Coppens, A. B., Frey, A. R., Kinsler, L. E., and Sanders, J. V., *Fundamentals of Acoustics, Third Edition*, John Wiley & Sons, Inc., Monterey, CA, 1980.

35. Interviews with C. S. Chiu and the author, May-June 1993.

36. Jensen, F. and Ferla, C., "Numerical Solutions of Range-Dependent Benchmark Problems in Ocean Acoustics", *J. Acoust. Soc. Am*, **87**(4), April 1990, pp. 1499–1510.

37. Math Works, Inc., *The Student Edition of MATLAB™*, Prentice Hall, Inc., Englewood Cliffs, New Jersey, 07632.

BIBLIOGRAPHY

Ansbro, A. P. and Arnold, J. M., "Numerically Efficient Evaluation of Intrinsic Modes in Wedge-Shaped Waveguides", *J. Acoust. Soc. Am.*, **89**(4), April, 1991.

Buckingham, M. J., *Acoustic Propagation in a Wedge Shaped Ocean with Perfectly Reflecting Boundaries*, NATO Advanced Research Workshop on a Hybrid Formulation of Wave Propagation and Scattering, 1983.

Buckingham, M. J., *Acoustic Propagation in a Wedge Shaped Ocean*, The A. B. Wood Memorial Lecture, Naval Research Lab, 1967 .

Buckingham, M. J., *Acoustic Propagation in a Wedge-Shaped Ocean with Perfectly Reflecting Boundaries*, Naval Research Laboratory Report 8797, 1984.

Buckingham, M. J., and Tolstoy, A., "An Analytical Solution for Benchmark Problem 1: The 'Ideal' Wedge", *J. Acoust. Soc. Am.*, **87**(4), April 1990.

Chwieroth, F. S., Nagl, A., Uberall, R. D., Groves, R. D., and Zarur, G. L., "Mode Coupling in a Sound Channel With Range-Dependent Parabolic Velocity Profile", *J. Acoust. Soc. Am*, **64**(4), 1978.

Collins, M. D., "Benchmark Calculations for Higher-Order Parabolic Equations", *J. Acoust. Soc. Am.*, **87**(4), April 1990.

Coppens, A. B., Humphries, M., and Sanders, J. V., "Propagation of Sound out of a Fluid Wedge into an Underlying Fluid Substrate of Greater Sound Speed", *J. Acoust. Soc. Am.*, **76**(5), November 1984.

Deane, G. B. and Tindle, C. T., "A Three Dimensional Analysis of Acoustic Propagation in a Penetrable Wedge Slice", *J. Acoust. Soc. Am.*, **92**(3), September 1992.

Desaubies, Y., "A Uniformly Valid Solution for Acoustic Normal Mode Propagation in a Range Varying Ocean", *J. Acoust. Soc. Am.*, **76**(2), 1976.

Evans, R. B., "The Decoupling of Stepwise Coupled Modes", *J. Acoust. Soc. Am.* **80**(5), 1986.

Felson, L. B., "Benchmarks: An Option for Quality Assessment", *J. Acoust. Soc. Am.*, **87**(4), April 1990.

Green, R. R., "The Rational Approximation to the Acoustic Wave Equation with Bottom Interaction", *J. Acoust. Soc. Am.*, **76**(6), December 1984.

Kamal, A., and Felson, L. B., "Spectral Theory of Sound Propagation in an Ocean Channel with Weakly Sloping Bottom," *J. Acoust. Soc. Am.*, **73**(4), April 1983.

Kuznetsov, V. K., "Emergence of Normal Modes Propagating in a Wedge on a Half-Space from the Former into the Latter", *Soviet Physical Acoustics*, **19**(3), 1973

Kuznetsov, V. K., "Method of Virtual Sources in the Underwater Acoustical Description of High-Frequency Sound Field in a Wedge", *Soviet Physical Acoustics*, **18**(2), 1972.

Lian S. W. and Pace, N. G., "Evaluations of the Analytic Solution for the Acoustic Field in an Ideal Wedge and the Approximate Solution in a Penetrable Wedge", *J. Acoust. Soc. Am.*, **89**(1), 1991.

McDaniel, S. T., "Mode Coupling Due to Interaction with the Seabed", *J. Acoust. Soc. Am.*, **72**(3), 1982.

Milder, D. M., "Ray and Wave Invariants for SOFAR Channel Propagation", *J. Acoust. Soc. Am.*, **46**(5), 1969.

Nagl, A., Uberall, H., Haug, A. J., and Zarur, G. L., "Adiabatic Mode Theory of Underwater Sound Propagation in a Range-Dependent Environment", *J. Acoust. Soc. Am.*, **63**(3), 1978.

Paliatsos, D., *Computer Studies of Sound Propagation in a Wedge-Shaped Ocean with Penetrable Bottom*, Master's Thesis, Naval Postgraduate School, Monterey, California, March 1989.

Pierce, A. D., "Guided Mode Disappearance During Upslope Propagation in Variable Depth Shallow Water Overlying a Fluid Bottom", *J. Acoust. Soc. Am.*, **72**(2), 1982.

Plumpton, N. G., and Tindle, C. T., "Saddle Point Analysis of the Reflected Acoustic Field", *J. Acoust. Soc. Am.*, **85**, 1989.

Stephen, R. A., "Solutions to Range-Dependent Benchmark Problems by the Finite-Difference Method", *J. Acoust. Soc. Am.*, **87**(4), April 1990.

Thomson, D. J., "Wide-Angle Parabolic Equation Solutions to Two Range-Dependent Benchmark Problems", *J. Acoust. Soc. Am.*, **87**(4), April 1990.

Westwood, E. K., "Ray Model Solutions to the Benchmark Wedge Problems", *J. Acoust. Soc. Am.*, **87**(4), April 1990.

Westwood, E. K., "The Modeling of a Shallow Water Wedge Using Complex Rays and Steepest-Descent Integration", *J. Acoust. Soc. Am.*, Supp 1, **83**, 1988.

INITIAL DISTRIBUTION LIST

		No. Copies
1.	Defense Technical Information Center Cameron Station Alexandria, VA 22304-6145	2
2.	Director, Submarine Warfare Division (N87) Chief of Naval Operations Washington, DC 20350-2000	1
3.	Library, Code 52 Naval Postgraduate School Monterey, CA 93943-5002	2
4.	Dr. A. B. Coppens, Code PH/Cz Department of Physics and Chemistry Naval Postgraduate School Monterey, CA 93943-5002	2
5.	Dr. J. V. Sanders, Code PH/Sd Department of Physics and Chemistry Naval Postgraduate School Monterey, CA 93943-5002	2
6.	Dr. C.S. Chiu, Code OC/Ci Department of Oceanography Naval Postgraduate School Monterey, CA 93943-5002	2
7.	LT C. C. Meisenheimer ASW Curriculum, Code 3A Naval Postgraduate School Monterey, CA 93943-1849	2